INFORMATION TO USERS

This reproduction was made from a copy of a document sent to us for microfilming. While the most advanced technology has been used to photograph and reproduce this document, the quality of the reproduction is heavily dependent upon the quality of the material submitted.

The following explanation of techniques is provided to help clarify markings or notations which may appear on this reproduction.

1. The sign or "target" for pages apparently lacking from the document photographed is "Missing Page(s)". If it was possible to obtain the missing page(s) or section, they are spliced into the film along with adjacent pages. This may have necessitated cutting through an image and duplicating adjacent pages to assure complete continuity.

2. When an image on the film is obliterated with a round black mark, it is an indication of either blurred copy because of movement during exposure, duplicate copy, or copyrighted materials that should not have been filmed. For blurred pages, a good image of the page can be found in the adjacent frame. If copyrighted materials were deleted, a target note will appear listing the pages in the adjacent frame.

3. When a map, drawing or chart, etc., is part of the material being photographed, a definite method of "sectioning" the material has been followed. It is customary to begin filming at the upper left hand corner of a large sheet and to continue from left to right in equal sections with small overlaps. If necessary, sectioning is continued again—beginning below the first row and continuing on until complete.

4. For illustrations that cannot be satisfactorily reproduced by xerographic means, photographic prints can be purchased at additional cost and inserted into your xerographic copy. These prints are available upon request from the Dissertations Customer Services Department.

5. Some pages in any document may have indistinct print. In all cases the best available copy has been filmed.

University Microfilms International
300 N. Zeeb Road
Ann Arbor, MI 48106

Order Number 1333228

Sensitivity of a frequency scanning program to variations in system resistances

Butt, Robert Samuel, Jr., M.S.

The University of Arizona, 1988

U·M·I
300 N. Zeeb Rd.
Ann Arbor, MI 48106

PLEASE NOTE:

In all cases this material has been filmed in the best possible way from the available copy. Problems encountered with this document have been identified here with a check mark __√__.

1. Glossy photographs or pages _____
2. Colored illustrations, paper or print ______
3. Photographs with dark background _____
4. Illustrations are poor copy ______
5. Pages with black marks, not original copy ______
6. Print shows through as there is text on both sides of page ______
7. Indistinct, broken or small print on several pages __√__
8. Print exceeds margin requirements ______
9. Tightly bound copy with print lost in spine ______
10. Computer printout pages with indistinct print ______
11. Page(s) __________ lacking when material received, and not available from school or author.
12. Page(s) __________ seem to be missing in numbering only as text follows.
13. Two pages numbered ______. Text follows.
14. Curling and wrinkled pages ______
15. Dissertation contains pages with print at a slant, filmed as received ________
16. Other ____

U·M·I

SENSITIVITY OF A FREQUENCY SCANNING PROGRAM TO VARIATIONS IN SYSTEM RESISTANCES

by

Robert Samuel Butt, Jr.

A Thesis Submitted to the Faculty of the

DEPARTMENT OF ELECTRICAL AND COMPUTER ENGINEERING

In Partial Fulfillment of the Requirements
For the Degree of

MASTER OF SCIENCE
WITH A MAJOR IN ELECTRICAL ENGINEERING

In the Graduate College

THE UNIVERSITY OF ARIZONA

1 9 8 8

STATEMENT BY AUTHOR

This thesis has been submitted in partial fulfillment of requirements for an advanced degree at The University of Arizona and is deposited in the University Library to be made available to borrowers under rules of the Library.

Brief quotations from this thesis are allowable without special permission, provided that accurate acknowledgment of source is made. Requests for permission for extended quotation from or reproduction of this manuscript in whole or in part may be granted by the head of the major department or the Dean of the Graduate College when in his or her judgment the proposed use of the material is in the interests of scholarship. In all other instances, however, permission must be obtained from the author.

SIGNED: Robert S. Butt, Jr.

APPROVAL BY THESIS CO-DIRECTORS

This thesis has been approved on the date shown below:

Larry C. Schooley — 2/19/88

Larry C. Schooley
Professor of Electrical Engineering — Date

James L. Knickerbocker — 2/19/88

James L. Knickerbocker, P.E.
Adjunct Professor of
Electrical Engineering — Date

ACKNOWLEDGMENTS

The author wishes to express his sincere gratitude to the following persons for their contributions to this thesis:

Baj L. Agrawal

Cesar E. Cruz

Richard G. Farmer

James L. Knickerbocker

Floyd L. Rose

Charles S. Russell

James F. Tang

Paul R. Vandiveer

A note of appreciation also to Barbara K. Wilson, who provided encouragement and support during the Fall of 1987.

TABLE OF CONTENTS

LIST OF ILLUSTRATIONS

LIST OF ILLUSTRATIONS--Continued

LIST OF TABLES

LIST OF TABLES--Continued

LIST OF TABLES--Continued

LIST OF TABLES--Continued

ABSTRACT

Various computer programs are currently used by electric utilities to determine if potential subsynchronous resonance problems exist which can impact turbine-generators. One of the most popular of these is the frequency scanning program. The representative transmission system input data for these programs are generally based on constant temperature and frequency. However, as conductor temperatures and applied frequencies fluctuate, the resistances also change. This thesis investigates the effects that resistance variations, due to temperature and frequency, have on frequency scanning results. The maximum resistance change (increased and decreased) from the standard value is determined and applied to the transmission lines in four study system cases. The frequency scan output data for the modified cases is used to determine if torsional interaction has become more severe. It is found that, under extreme conditions, the net system damping can decrease by over one hundred percent.

CHAPTER ONE

INTRODUCTION

The theory of subsynchronous resonance (SSR) in electric power systems first appeared in the technical literature in 1937[1]. Several papers addressing the subject were published during the following thirty years, but the serious consequences of SSR were not fully realized until the early 1970's, when two turbine-generator shaft failures occurred at Mohave Generating Station in southern Nevada. Electric utilities in the Southwestern United States are now spending millions of dollars to avoid undesirable interaction between mechanical and electrical systems. This SSR interaction may occur when series capacitors are placed in long transmission lines to compensate for the inductive reactance which is inherent to the lines.

Definition of Resonance

Resonance is defined[4] by the Institute of Electrical and Electronics Engineers (IEEE) as the

---

[1] J. W. Butler and C. Concordia, "Analysis of Series Capacitor Application Problems," (1937).

[4] IEEE Standard Dictionary of Electrical and Electronics Terms, (1977).

enhancement of the response of a physical system to a periodic excitation when the excitation frequency is equal to a natural frequency of the system.

Resonance in electrical power systems may occur at many different frequencies, depending upon system configurations and operating conditions. Subsynchronous resonance, in the electrical sense, implies a resonance condition which occurs below the normal power system operating frequency of 60 Hz. Of concern in SSR studies is the interaction between resonant electrical and mechanical systems.

SSR Problems - The Mohave Incident

In the American Southwest, where many generating stations are located at substantial distances from load centers, high voltage transmission lines traverse hundreds of miles. The high inductive reactances which are present in the transmission systems limit the transfer capability of the lines. Series capacitors have been utilized as an effective and economical means for reducing the line inductive reactance. However, the presence of these capacitors may result in subsynchronous resonance problems and costly damage to turbine-generator shafts.

The implications of subsynchronous resonance (SSR) became apparent when two shaft failures were experienced by the Southern California Edison Company at Mohave Generating Station in December 1970 and October 1971. The Mohave failures were extensively analyzed[9] and have been attributed to an interaction between the series capacitor-compensated transmission system and one of the natural torsional modes of the turbine-generator.

Analysis of line current oscillograms taken during the Mohave disturbance revealed the presence of appreciable currents of subsynchronous frequency. In general, these subsynchronous currents do not cause any harm to the electrical system, but they will flow in the armatures of rotating machinery and react with magnetic flux. The interaction between the subsynchronous stator currents and the rotor field flux rotating at synchronous speed will result in air gap torques on the rotor system at slip frequencies which are the difference between the synchronously rotating main generator flux and the subsynchronous currents flowing in the electrical network. The subsynchronous stator current frequency and the corresponding frequency of the oscillating torques are thus

---

[9] D. N. Walker, C. E. J. Bowler, R. L. Jackson and D. A. Hodges, "Results of Subsynchronous Resonance Test at Mohave," (1975).

synchronous (60 Hz) complements of one another. If the applied torques happen to correspond closely to any of the torsional modal frequencies of the turbine-generator system, the resulting rotor motions can become appreciable and the corresponding shaft torques that develop can be damaging.

The 60 Hz complement frequency of the line currents which were present at both of the Mohave failures very nearly coincided with the second torsional mode of the turbine-generator rotor system, resulting in an unstable condition referred to as torsional interaction.

Types Of SSR

SSR phenomena are generally classified as being either transient or steady state. Transient SSR refers to transient torques on segments of turbine-generator shafts resulting from subsynchronous oscillating currents in the electrical network caused by faults or switching operations. Steady state SSR, also known as self-excited SSR, involves subsynchronous oscillations that are either sustained or increase in magnitude with time. These oscillations originate in the electrical system as a result of the R-L-C circuit configuration and system operating conditions, and can lead to self-excited oscillations in the mechanical system.

The two forms of self-excited SSR are the induction generator effect which involves electrical system dynamics only, and the torsional interaction effect which involves both the electrical and mechanical system dynamics. The result of each of these effects is such that the generator appears as a negative resistance.

Techniques for Evaluating SSR

Several techniques are currently available for SSR studies. Three of the most common methods used to analyze power system networks for SSR are:

1. Time Simulation
2. Eigenvalue Analysis
3. Frequency Scanning Analysis

The Electromagnetic Transients Program (EMTP) is a time simulation technique which is commonly used for examining the transient shaft torques which result from abrupt changes within an electrical system. The Eigenvalue and frequency scanning methods are used primarily for the study of self-excitation. Eigenvalue analysis accurately provides all the natural modes in the system, but this technique is relatively expensive and becomes cumbersome when there are more than 20 buses in the study system. Frequency scanning has become the workhorse of the industry for most SSR studies, and is an approximate but cost-effective method for determining potential SSR problems. A frequency scan output plot contains the effective system impedance as viewed from the generator neutral over a frequency range of interest.

RESOUT is a frequency scanning program originally developed by General Electric and currently used by numerous Southwestern power utilities. RESOUT was obtained by Salt River Project (SRP), a Phoenix utility, after several modifications by other power companies. Additional enhancements were made to the program, and the SRP version is now called SRPRES. More information on the background of SRPRES is presented in Appendix B. The program calculates the SSR impedance of the electrical system, viewed from the neutral of the generator under study, as a function of frequency. For each frequency, the manufacturer-supplied induction generator impedance is combined with the calculated network driving point impedance, resulting in an effective system impedance. This combination of the network driving point impedance and the machine impedance is known as SSR impedance.

Frequency Scanning Applications

A frequency scan output plot contains the calculated SSR impedance values versus frequency. Agrawal and Farmer (1979) showed that inspection of these plots can reveal information about potential induction generator and transient torque problems. A resonant condition is determined where the SSR reactance reaches zero or a local minimum value. At each electrical resonant frequency, if the SSR resistance is negative and a series resonance exists, an induction generator problem is indicated. A quick test for transient torque problems can be accomplished by inspecting the slope of the SSR reactance curve near the 60 Hz complements of the machine modal frequencies. If there is at least a 5 percent reactance dip within 3 Hz of these frequencies, a possible transient torque problem exists.

In addition to being useful for locating potential induction generator and transient torque problems, the information obtained from SRPRES may also be used to determine if a torsional interaction problem is present[14]. The output of SRPRES includes values of SSR resistance and reactance versus frequency. The program also provides the conductance (G) of the electrical system (including the generator), for each frequency. The conductance at a

---

[14] B. L. Agrawal and R. G. Farmer, "Use of Frequency Scanning Techniques for Subsynchronous Resonance Analysis," (1979).

machine modal frequency (G_n), together with the stored machine inertial energy (H_n) and the modal frequency (f_n) are used to determine the amount of undamping at the n-th torsional mode by the equation

$$\triangle\sigma_n = [(60-f_n)/(8*f_n*H_n)]*G_n, \qquad (1)$$

where H_n and G_n are per unit quantities on a common MVA base.

The SSR conductance at a particular mode can be expressed in terms of the SSR resistance and SSR reactance by the equation

$$G_n = \text{SSR R}/(\text{SSR R}^2 + \text{SSR X}^2) \qquad (2)$$

Inspection of Equation 2 reveals that, for a constant value of X, the value of G_n will be a maximum when R = X. Further, when R is less than X, an increase in R will lead to an increase in G_n. Conversely, when R is greater than X, an increase in R will lead to a decrease in G_n.

When the machine damping, (σ_n), at a particular modal frequency and level of machine loading is known, the net damping, (σ_{NET}), may be determined by the equation

$$\sigma_{NET} = \sigma_n - \triangle\sigma_n \qquad (3)$$

If the calculated undamping exceeds the machine damping at a particular modal frequency (net damping becomes negative), instability due to torsional interaction is indicated.

The undamping which is determined for each torsional mode indicates to the engineer the amount of damping which may be required to stabilize the system. The accuracy of these calculated undamping values is dependent upon the accuracy of the input data to the frequency scanning program. If transmission line parameters change, the input data should change accordingly. The resistance values which are used for the input data are typically based on 25°C and 60 Hz. However, as conductor loading and meteorological conditions change over the course of a year, the corresponding conductor temperatures will fluctuate about the 25°C value by a substantial amount. In addition, the presence of harmonics and transients results in a variety of frequencies in the power system network, thus leading to a change in resistance due to skin effect from the normal 60 Hz value. As a result, the value of resistance for a transmission line may vary significantly, and this can have an adverse effect on the results of a frequency scanning study. An engineer may determine that a generating station is safe from SSR problems based on the results of a frequency scanning study, when in reality the turbine-generator may be susceptible to SSR torsional interaction under extreme weather conditions and/or system operating conditions.

Overview

The purpose of this study is to determine the effects of variations in transmission system resistances on the results of frequency scanning studies. The study cases include two existing transmission systems in Arizona, and two systems which were presented in IEEE papers for the study of subsynchronous resonance. Chapter Two will examine the changes in resistance with temperature and frequency for 2156 MCM ACSR conductor, which is commonly used in extra-high voltage transmission systems. In Chapter Three, the maximum variations in resistance will be applied to the line resistances in the study cases and the modified cases will be subjected to frequency scans. The values of undamping and net damping for each mode will be calculated using the output data from these cases and Equations 1 and 3. These values will be compared to those obtained from 25°C, 60 Hz frequency scans.

CHAPTER TWO

TRANSMISSION SYSTEM RESISTANCES

Electrical power loss in a transmission line is directly proportional to the electrical resistance of the conductor used. The resistance depends on the electrical conductivity of the strands, the cross-sectional area and temperature of the conductor and, for AC lines, whether or not the conductor material is ferromagnetic.

DC Resistance of a Stranded Conductor

The DC resistance of a stranded conductor is a function of its area, conductivity, lay lengths and temperature. Over moderate ranges of temperature the change of resistance in a conductor is proportional to the change of temperature[23]. In general, if R_{t1} is the resistance of a conductor at a temperature t1, and α_{t1} is the temperature coefficient at that temperature, the resistance at some other temperature t2 is expressed by the formula[22]

$$R_{t2}=R_{t1}*[1+\alpha_{t1}*(t2-t1)] \quad (4)$$

[23] Standard Handbook for Electrical Engineers, (1978).

[22] Task Force of the IEEE Working Group on Calculation of Bare Overhead Conductor Temperatures, "AC Resistance of ACSR - Magnetic and Temperature Effects," (1985).

Effects of Temperature Variations

The mean ambient high and low temperatures in January and July for the geographic areas which include some of the transmission lines in this study are shown in Table 1. Also shown are the record temperature extremes for Payson and St. Johns, Arizona. These data are based on the 30-year period from 1951 to 1980. From this table, it can be seen that the record high for Payson was 42°C, while the record low was -22°C.

TABLE 1 - SELECTED MONTHLY MEAN AND RECORD TEMPERATURES(°C)

Station	January High/Low	July High/Low	Record High/Low
Flagstaff	6/-9	28/10	
Lee's Ferry	9/-3	40/23	
Payson	12/-4	34/14	42/-22
St. Johns	9/-8	33/14	39/-34
Winslow	7/-7	34/17	
Colorado City	8/-6	34/16	

For this study, the transmission lines will be subjected to ambient temperature extremes which are assumed to range from a low of -7°C to a high of 25°C. In addition, severe ambient situations will be studied in which the ambient temperature drops to -22°C and increases to 42°C. This is a realistic assumption for Arizona, where wide ambient temperature ranges exist.

The operating temperature of a conductor is a function of the ambient temperature, the cross-wind velocity, the current through the conductor, and the amount of solar radiation striking the conductor. It has been found[22] that, for an ambient temperature of 25°C, a conductor surface temperature of approximately 75°C is obtained with a current of 1800 amps for 2156 MCM ACSR. This is for full-load conditions with negligible cross-wind. If the ambient temperature were 42°C under full load conditions and negligible cross-wind, the conductor operating temperature will be even higher. Conversely, if the line is lightly loaded and a strong cross-wind is present (20 mph), the conductor temperature can be as cold as, if not colder than, the ambient temperature (i.e., when moisture is present).

The extreme cases for conductor temperature will be assumed for this study. For the low ambient temperature of -7°C and the severe case ambient temperature of -22°C, the conductor will be lightly loaded with a strong cross-wind at night. The conductor temperature under these conditions will be assumed to be the same as the ambient. For an ambient temperature of 25°C, the conductor will be fully-loaded with negligible cross-wind during the

---

[22]Task Force of the IEEE Working Group on Calculation of Bare Overhead Conductor Temperatures, "AC Resistance of ACSR - Magnetic and Temperature Effects," (1985).

afternoon. The conductor temperature at 25°C ambient will be 75°C. A severe case ambient temperature of 42°C with a fully-loaded conductor temperature of 100°C is also studied.

All transmission lines in this study are 2156 MCM ACSR. The DC resistance of 2156 MCM steel-reinforced aluminum conductor at 25°C, as determined by the Electric Power Research Institute[24], is 0.0426 ohms per mile. The temperature coefficient for aluminum (61 % conductivity) at 25°C is 0.00395[23]. With this information, Equation 4 was used to calculate the DC resistance of this conductor at 75°C, 100°C, -7°C, and -22°C, and the corresponding resistances are shown in Table 2.

TABLE 2 - CHANGE IN DC RESISTANCE WITH TEMPERATURE

Conductor Temp.	Resistance - ohms/mile
25°C	0.0426
75°C	0.0510
100°C	0.0552
-7°C	0.0372
-22°C	0.0347

From Table 2, the DC resistance at the conductor temperature extremes is seen to increase by as much as

---

[24]Electric Power Research Institute, Transmission Line Reference Book, (1982), p.110.

[23]Standard Handbook for Electrical Engineers, (1978), p.4-9.

22.5% at 100°C and decrease by 18.5% at -22°C from the 25°C value.

AC Resistance of a Stranded Conductor

In any conductor carrying alternating current, the magnetic field around the axis of the conductor produces variations in the current density[18]. In an isolated conductor, the current tends to flow more densely in the outermost parts, farthest from the axis of the conductor. The effect is more pronounced as the frequency becomes high, and the current becomes concentrated in the outer skin of the conductor - hence the name "skin effect".

The change of resistance due to skin effect may be determined fairly easily by use of the appropriate sets of tables and equations as follows[23]: If R_{DC} is the DC resistance of a linear cylindrical conductor, then R_{eff}, the effective resistance to AC current of a given frequency, can be determined by the equation

$$R_{eff} = K_1 * R_{DC} \quad , \tag{5}$$

where K_1 is a constant which is determined from a table for a certain value of K_2. Table 5 shows the corresponding

---

[18] H. B. Dwight, "Skin Effect in Tubular and Flat Conductors," (1918).

[23] Standard Handbook for Electrical Engineers, (1978).

values of K_1 for K_2. For practical calculation, the value of K_2 is given by

$$K_2=0.063598*[(f*\mu/R_{DC})^{1/2}], \qquad (6)$$

where f is the frequency in cycles per second, μ is the magnetic permeability of the conductor (assumed constant), and R_{DC} is the DC resistance of the conductor in ohms per mile at the operating temperature. For nonmagnetic materials, such as copper and aluminum, the permeability is equal to 1.

Effects of Frequency Variations

Equations 5 and 6 will be now used to determine the change in resistance for the various electrical frequencies which may be present. The frequencies of interest will be the 60 Hz complements of the torsional modal frequencies for the turbine-generators under study. Four total generators are studied, and the electrical frequencies which correspond to the generator torsional modal frequencies range from a low of 8.9 Hz for the GEN1 generator in System C and System D, to a high frequency of 44.29 Hz for the Navajo generator in System B. The 60 Hz complements for the torsional modal frequencies of the generators in this study are shown in Table 3.

TABLE 3 - GENERATOR ELECTRICAL FREQUENCIES CORRESPONDING TO TORSIONAL MODAL FREQUENCIES

Generator	Mode	Modal Freq. (f_n)	Electrical Freq. (f_e)
Coronado	1	33.4	26.6
(System A)	2	44.7	15.3
Navajo	1	15.71	44.29
(System B)	2	20.21	39.79
	3	25.55	34.45
	4	32.28	27.72
GEN1	1	24.65	35.35
(System C,	2	32.39	27.61
System D)	3	51.1	8.9
GEN2	1	24.65	35.35
(System D)	2	44.99	15.01

It has been shown that temperature can affect the resistance of a conductor. The resistance may also change due to skin effect. The resistances of 2156 MCM ACSR for several frequencies were calculated and are shown in Table 4. For a DC resistance of .0426 ohms/mile, the resistance of the conductor at a frequency of 8.9 Hz is 12.7% less than the resistance at 60 Hz. Further, when the DC resistance is .0347 ohms/mile, the resistance at 8.9 Hz is 17.1% less than the 60 Hz value. Thus, skin effect depends upon the DC resistance of the conductor as well as the applied frequency.

The electrical frequencies of Table 3 will be used in determining the conductor resistance including skin effect. These frequencies will be assumed for a torsional interaction condition at a particular mode.

TABLE 4 - RESISTANCE CHANGES FOR SELECTED FREQUENCIES

R_{DC}	$R_{8.9}$	$R_{15.3}$	$R_{27.7}$	$R_{35.4}$	R_{60}
.0426	.0428	.0431	.0441	.0450	.0490
.0552	.0553	.0556	.0564	.0571	.0604
.0347	.0349	.0353	.0365	.0376	.0421

Equation 6 was used to determine values of K_2 for the corresponding frequencies in each study system. After the values of K_2 were obtained, the corresponding values of K_1 were determined using Table 5[23] and interpolating. The resulting values of K_1 and K_2 are shown in Tables 6 through 10. At 25°C, the value of K_2 at 60 Hz is 2.3868. From Table 5, this corresponds to a K_1 value of 1.1492. The standard value of resistance for 2156 MCM conductor is thus 0.0426*1.1492=0.04896 ohms per mile (at 60 Hz).

TABLE 5 - SKIN EFFECT RATIOS

K_2	K_1	K_2	K_1	K_2	K_1	K_2	K_1
0.5	1.00032	1.1	1.00758	1.7	1.04205	2.3	1.13069
0.6	1.00067	1.2	1.01071	1.8	1.05240	2.4	1.15207
0.7	1.00124	1.3	1.01470	1.9	1.06440	2.5	1.17538
0.8	1.00212	1.4	1.01969	2.0	1.07816	2.6	1.20056
0.9	1.00340	1.5	1.02582	2.1	1.09375	2.7	1.22753
1.0	1.00519	1.6	1.03323	2.2	1.11126	2.8	1.25620

---

[23] Standard Handbook for Electrical Engineers, (1978), p.4-28.

TABLE 6 - VALUES OF K_1,K_2 FOR SYSTEM A

T,°C	R_{DC}	K_2 (f_e = 26.6 Hz)	K_1 (f_e = 26.6 Hz)	K_2 (f_e = 15.3 Hz)	K_1 (f_e = 15.3 Hz)
75	0.0510	1.4524	1.0229	1.1015	1.0076
100	0.0552	1.3961	1.0195	1.0588	1.0066
-7	0.0372	1.7006	1.0421	1.2898	1.0143
-22	0.0347	1.7608	1.0483	1.3354	1.0165

TABLE 7 - VALUES OF K_1,K_2 FOR SYSTEM B

(44.29 Hz & 39.79 Hz)

T,°C	R_{DC}	K_2 (f_e = 44.29 Hz)	K_1 (f_e = 44.29 Hz)	K_2 (f_e = 39.79 Hz)	K_1 (f_e = 39.79 Hz)
75	0.0510	1.8742	1.0613	1.7764	1.0500
100	0.0552	1.8015	1.0526	1.7075	1.0428
-7	0.0372	2.1944	1.1103	2.0800	1.0906
-22	0.0347	2.2721	1.1253	2.1536	1.1031

TABLE 8 - VALUES OF K_1,K_2 FOR SYSTEM B

(34.45 Hz & 27.72 Hz)

T,°C	R_{DC}	K_2 (f_e = 34.45 Hz)	K_1 (f_e = 34.45 Hz)	K_2 (f_e = 27.72 Hz)	K_1 (f_e = 27.72 Hz)
75	0.0510	1.6529	1.0379	1.4827	1.0248
100	0.0552	1.5888	1.0324	1.4252	1.0212
-7	0.0372	1.9354	1.0693	1.7361	1.0458
-22	0.0347	2.0039	1.0788	1.7975	1.0521

TABLE 9 - VALUES OF K_1,K_2 FOR SYSTEMS C & D - GEN1

T,°C	R_{DC}	K_2 (f_e = 35.35 Hz)	K_1 (f_e = 35.35 Hz)	K_2 (f_e = 27.61 Hz)	K_1 (f_e = 27.61 Hz)	K_2 (f_e = 8.9 Hz)	K_1 (f_e = 8.9 Hz)
75	0.0510	1.6744	1.0398	1.4798	1.0246	0.8401	1.0026
100	0.0552	1.6094	1.0341	1.4224	1.0211	0.8075	1.0022
-7	0.0372	1.9605	1.0727	1.7326	1.0454	0.9837	1.0049
-22	0.0347	2.0299	1.0828	1.7940	1.0518	1.0185	1.0056

TABLE 10 - VALUES OF K_1,K_2 FOR SYSTEM D - GEN2

T,°C	R_{DC}	K_2 (f_e = 35.35 Hz)	K_1 (f_e = 35.35 Hz)	K_2 (f_e = 15.01 Hz)	K_1 (f_e = 15.01 Hz)
75	0.0510	1.6744	1.0398	1.0911	1.0074
100	0.0552	1.6094	1.0341	1.0487	1.0064
-7	0.0372	1.9605	1.0727	1.2775	1.0138
-22	0.0347	2.0299	1.0828	1.3227	1.0158

The effects of frequency on the resistances of this study may now be determined using equation 5. The corresponding resistances for the K_1 values presented in Tables 6 through 10 were calculated and are shown in Tables 11 through 16 (ohms per mile). Also shown are the percent changes in resistance from the standard 60 Hz, 25°C value (I for an increase in resistance, D for a decrease).

TABLE 11 - VARIATIONS IN RESISTANCE WITH FREQUENCY FOR SYSTEM A

		f_e=26.6 Hz			f_e=15.3 Hz		
T,°C	R_{DC}	K_1	R_{eff}	%Change	K_1	R_{eff}	%Change
75	0.0510	1.0229	0.0522	6.6 I	1.0076	0.0514	5.0 I
100	0.0552	1.0195	0.0563	15.0 I	1.0066	0.0556	13.6 I
-7	0.0372	1.0421	0.0388	20.8 D	1.0143	0.0377	23.0 D
-22	0.0347	1.0483	0.0364	25.7 D	1.0165	0.0353	27.9 D

TABLE 12 - VARIATIONS IN RESISTANCE WITH FREQUENCY FOR SYSTEM B (44.29 Hz & 39.79 Hz)

		f_e=44.29 Hz			f_e=39.79 Hz		
T,°C	R_{DC}	K_1	R_{eff}	%Change	K_1	R_{eff}	%Change
75	0.0510	1.0613	0.0541	10.5 I	1.0500	0.0536	9.5 I
100	0.0552	1.0526	0.0581	18.7 I	1.0428	0.0576	17.6 I
-7	0.0372	1.1103	0.0413	15.6 D	1.0906	0.0406	17.1 D
-22	0.0347	1.1253	0.0390	20.3 D	1.1031	0.0383	21.8 D

TABLE 13 - VARIATIONS IN RESISTANCE WITH FREQUENCY FOR SYSTEM B (34.45 Hz & 27.72 Hz)

		f_e=34.45 Hz			f_e=27.72 Hz		
T,°C	R_{DC}	K_1	R_{eff}	%Change	K_1	R_{eff}	%Change
75	0.0510	1.0379	0.0529	8.0 I	1.0248	0.0523	6.8 I
100	0.0552	1.0324	0.0570	16.4 I	1.0212	0.0564	15.2 I
-7	0.0372	1.0693	0.0398	18.7 D	1.0458	0.0389	20.5 D
-22	0.0347	1.0788	0.0374	23.6 D	1.0521	0.0365	25.4 D

TABLE 14 - VARIATIONS IN RESISTANCE WITH FREQUENCY FOR SYSTEMS C & D - GEN1 (35.35 Hz & 27.61 Hz)

		f_e=35.35 Hz			f_e=27.61 Hz		
T,°C	R_{DC}	K_1	R_{eff}	%Change	K_1	R_{eff}	%Change
75	0.0510	1.0398	0.0530	8.3 I	1.0246	0.0523	6.8 I
100	0.0552	1.0341	0.0571	16.6 I	1.0211	0.0564	15.2 I
-7	0.0372	1.0727	0.0399	18.5 D	1.0454	0.0389	20.5 D
-22	0.0347	1.0828	0.0376	23.2 D	1.0518	0.0365	25.4 D

TABLE 15 - VARIATIONS IN RESISTANCE WITH FREQUENCY FOR SYSTEMS C & D - GEN1 (8.9 Hz)

f_e=8.9 Hz

T,°C	R_{DC}	K_1	R_{eff}	%Change
75	0.0510	1.0026	0.0511	4.4 I
100	0.0552	1.0022	0.0553	12.9 I
-7	0.0372	1.0049	0.0374	23.6 D
-22	0.0347	1.0056	0.0349	28.7 D

TABLE 16 - VARIATIONS IN RESISTANCE WITH FREQUENCY FOR SYSTEM D - GEN2

		f_e=35.35 Hz			f_e=15.01 Hz		
T,°C	R_{DC}	K_1	R_{eff}	%Change	K_1	R_{eff}	%Change
75	0.0510	1.0398	0.0530	8.3 I	1.0074	0.0514	5.0 I
100	0.0552	1.0341	0.0571	16.6 I	1.0064	0.0556	13.6 I
-7	0.0372	1.0727	0.0399	18.5 D	1.0138	0.0377	23.0 D
-22	0.0347	1.0828	0.0376	23.2 D	1.0158	0.0352	28.1 D

The data presented in Tables 11 through 16 will be applied in Chapter Three to the transmission system resistances in the study cases. There are two basic assumptions. The first is that constant conductor temperatures exist throughout the entire transmission system. Secondly, the frequencies of concern will be the 60 hertz complement frequencies of the machine torsional modes where torsional interaction is taking place.

CHAPTER THREE

EFFECTS OF RESISTANCE VARIATIONS ON FREQUENCY SCANNING RESULTS

At any given generating station location it is likely that the electrical system natural frequencies will vary considerably over a period of time, depending on the total electrical system topography and operating conditions. Changes in the system may result from transmission line outages, number and capacity of generators on-line, and the amount of series compensation in the lines. With the wide range of frequencies present in transmission systems, the change in resistance of conductors due to skin effect will vary, depending upon the physical characteristics of the conductors and the applied frequencies. In addition, system resistances will fluctuate with the meteorological conditions such as heavy winds, humidity and ambient temperature extremes over the course of a year.

The effects of temperature and frequency on the resistance of 2156 MCM ACSR conductor for the assumed conditions were determined in Chapter Two. These resistance variations will now be applied to the cases in this study.

Applications to the Study Systems

Four different systems will be studied. System A consists of a portion of the Coronado transmission system in eastern Arizona, and includes a radial tie between Coronado Generating Station and Cholla Generating Station, with five additional lines emanating from the Cholla station. The System A configuration is vulnerable to both series and parallel resonance conditions. System B comprises the Navajo Generating Station in northern Arizona and one transmission line connected to a remote transmission station nearly 275 miles away. System C and System D are both parallel impedance systems that were presented in an IEEE paper (First Benchmark Paper, 1985) for SSR analysis.

The results of Chapter Two will now be applied to the base cases. Tables 11 through 16 showed the change, in percent, of 2156 MCM conductor at various temperatures for the electrical frequencies of concern. All resistance values in the study cases were adjusted by these percentages, and the line resistances corresponding to these modifications are shown in Tables 17 through 32 (values in p.u.). The lines which were adjusted are shown in the single line diagrams and input data listings of Appendix A.

TABLE 17 - MODIFIED LINE RESISTANCES IN SYSTEM A (75°C & 100°C)

		75°C		100°C	
Line #	25°C,60 Hz	26.6 Hz	15.3 Hz	26.6 Hz	15.3 Hz
19	0.0083	0.00885	0.00872	0.00955	0.00943
20	0.0083	0.00885	0.00872	0.00955	0.00943
21	0.0069	0.00736	0.00725	0.00794	0.00784
22	0.0069	0.00736	0.00725	0.00794	0.00784
24	0.0007	0.00075	0.00074	0.00081	0.00080
39	0.0020	0.00213	0.00210	0.00230	0.00227

TABLE 18 - MODIFIED LINE RESISTANCES IN SYSTEM A (-7°C & -22°C)

		-7°C		-22°C	
Line #	25°C,60 Hz	26.6 Hz	15.3 Hz	26.6 Hz	15.3 Hz
19	0.0083	0.00657	0.00639	0.00617	0.00598
20	0.0083	0.00657	0.00639	0.00617	0.00598
21	0.0069	0.00546	0.00531	0.00513	0.00497
22	0.0069	0.00546	0.00531	0.00513	0.00497
24	0.0007	0.00055	0.00054	0.00052	0.00050
39	0.0020	0.00158	0.00154	0.00149	0.00144

TABLE 19 - MODIFIED LINE RESISTANCES IN SYSTEM B (75°C)

Line #	25°C,60 Hz	44.29 Hz	39.79 Hz	34.45 Hz	27.72 Hz
3	0.002241	0.002476	0.002454	0.002420	0.002393

TABLE 20 - MODIFIED LINE RESISTANCES IN SYSTEM B (100°C)

Line #	25°C,60 Hz	44.29 Hz	39.79 Hz	34.45 Hz	27.72 Hz
3	0.002241	0.002660	0.002635	0.002609	0.002582

TABLE 21 - MODIFIED LINE RESISTANCES IN SYSTEM B (-7°C)

Line #	25°C,60 Hz	44.29 Hz	39.79 Hz	34.45 Hz	27.72 Hz
3	0.002241	0.001891	0.001858	0.001822	0.001782

TABLE 22 - MODIFIED LINE RESISTANCES IN SYSTEM B (-22°C)

Line #	25°C,60 Hz	44.29 Hz	39.79 Hz	34.45 Hz	27.72 Hz
3	0.002241	0.001786	0.001752	0.001712	0.001672

TABLE 23 - MODIFIED LINE RESISTANCES IN SYSTEM C (75°C)

Line #	25°C,60 Hz	35.35 Hz	27.61 Hz	8.9 Hz
3	0.0074	0.008014	0.007903	0.007726
4	0.0067	0.007256	0.007156	0.006995
5	0.0014	0.001516	0.001495	0.001462

TABLE 24 - MODIFIED LINE RESISTANCES IN SYSTEM C (100°C)

Line #	25°C,60 Hz	35.35 Hz	27.61 Hz	8.9 Hz
3	0.0074	0.008628	0.008525	0.008355
4	0.0067	0.007812	0.007718	0.007564
5	0.0014	0.001632	0.001613	0.001581

TABLE 25 - MODIFIED LINE RESISTANCES IN SYSTEM C (-7°C)

Line #	25°C,60 Hz	35.35 Hz	27.61 Hz	8.9 Hz
3	0.0074	0.006031	0.005883	0.005654
4	0.0067	0.005461	0.005327	0.005119
5	0.0014	0.001141	0.001113	0.001070

TABLE 26 - MODIFIED LINE RESISTANCES IN SYSTEM C (-22°C)

Line #	25°C,60 Hz	35.35 Hz	27.61 Hz	8.9 Hz
3	0.0074	0.005683	0.005520	0.005276
4	0.0067	0.005146	0.004998	0.004777
5	0.0014	0.001075	0.001044	0.000998

TABLE 27 - MODIFIED LINE RESISTANCES IN SYSTEM D - GEN1 (75°C)

Line #	25°C,60 Hz	35.35 Hz	27.61 Hz	8.9 Hz
5	0.0052	0.005632	0.005554	0.005429
6	0.0014	0.001516	0.001495	0.001462

TABLE 28 - MODIFIED LINE RESISTANCES IN SYSTEM D - GEN1 (100°C)

Line #	25°C,60 Hz	35.35 Hz	27.61 Hz	8.9 Hz
5	0.0052	0.006063	0.005990	0.005871
6	0.0014	0.001632	0.001613	0.001581

TABLE 29 - MODIFIED LINE RESISTANCES IN SYSTEM D - GEN1 (-7°C)

Line #	25°C,60 Hz	35.35 Hz	27.61 Hz	8.9 Hz
5	0.0052	0.004238	0.004134	0.003973
6	0.0014	0.001141	0.001113	0.001070

TABLE 30 - MODIFIED LINE RESISTANCES IN SYSTEM D - GEN1 (-22°C)

Line #	25°C,60 Hz	35.35 Hz	27.61 Hz	8.9 Hz
5	0.0052	0.003994	0.003879	0.003708
6	0.0014	0.001075	0.001044	0.000998

TABLE 31 - MODIFIED LINE RESISTANCES IN SYSTEM D - GEN2
(75°C & 100°C)

		75°C		100°C	
Line #	25°C,60 Hz	35.35 Hz	15.01 Hz	35.35 Hz	15.01 Hz
5	0.0052	0.005632	0.005460	0.006063	0.005907
6	0.0014	0.001516	0.001470	0.001632	0.001590

TABLE 32 - MODIFIED LINE RESISTANCES IN SYSTEM D - GEN2
(-7°C & -22°C)

		-7°C		-22°C	
Line #	25°C,60 Hz	35.35 Hz	15.01 Hz	35.35 Hz	15.01 Hz
5	0.0052	0.004238	0.004004	0.003994	0.003739
6	0.0014	0.001141	0.001078	0.001075	0.001007

The modified cases were subjected to frequency scans by the program SRPRES. The values of SSR resistance, reactance, and maximum conductance values for each of the cases in System A are shown in Table 33.

TABLE 33 - FREQUENCY SCAN OUTPUT DATA FOR SYSTEM A

	f_e=26.6 Hz			f_e=15.3 Hz		
T,°C	R	X	G	R	X	G
25	.00345	.03818	2.3457	.01405	.01797	26.9968
75	.00359	.03827	2.4321	.01397	.01809	26.7419
100	.00377	.03838	2.5333	.01383	.01828	26.3264
-7	.00295	.03790	2.0410	.01449	.01740	28.2551
-22	.00283	.03783	1.9644	.01459	.01727	28.5449

The following observations can be made of Table 33:

1. In mode 1 (f_e=26.6 Hz), the SSR resistance and conductance increase and decrease with temperature.
2. In mode 2 (f_e=15.3 Hz), the SSR resistance and conductance decrease as temperature increases and increase as temperature decreases.
3. The SSR reactance increases and decreases with temperature in both modes.

Maximum undamping values at the 60 Hz complement frequencies, corresponding to particular levels of series compensation, were calculated using Equation 1. The net system damping, σ_{NET}, was then determined using Equation 3 and the value of machine no load damping, σ_n. The net damping for the modified cases was compared to the net damping for the 25°C, 60 Hz case, and the percent change was determined for the cases where the net damping decreased. A decrease in net damping indicates that the system is becoming less stable. The results of the calculations for undamping and net damping for the Coronado system (System A), are shown in Table 34.

TABLE 34 - MAXIMUM UNDAMPING AND NET DAMPING COMPARISON SYSTEM A

	Mode 1 (σ_1=0.042)			Mode 2 (σ_2=0.029)		
	f_e=26.6 Hz			f_e=15.3 Hz		
	cap.5=25%, cap.6=37.5%, cap.7=cap.8=16%			cap.5=25%, cap.6=37.5% cap.7=24%, cap.8=40%		
T,°C	$\Delta\sigma_1$(max)	σ_{NET}	% Dec.	$\Delta\sigma_2$(max)	σ_{NET}	% Dec.
25	0.01150	0.0305	-	0.02565	0.0034	-
75	0.01192	0.0301	1.3	0.02540	0.0036	-
100	0.01241	0.0296	3.0	0.02500	0.0040	-
-7	0.01000	0.0320	-	0.02684	0.0022	35.3
-22	0.00963	0.0324	-	0.02712	0.0019	44.1

The Coronado generator in System A is tied to the Cholla station via one transmission line. Several series compensated lines emanate from Cholla to the remainder of the electrical system. System A can thus contain both series and parallel resonances. From Table 34, the net damping decreases for mode 1 when the system resistances increase due to temperature (75°C and 100°C). A decrease in the net damping for mode 2 occurs when the system resistances decrease due to temperature (-7°C and -22°C).

The frequency scan output data for the cases of System B (for maximum conductance values) are shown in Tables 35 and 36.

TABLE 35 - FREQUENCY SCAN OUTPUT DATA FOR SYSTEM B (44.3 & 39.8 Hz)

	f_e=44.3 Hz			f_e=39.8 Hz		
T,°C	R	X	G	R	X	G
25	.00045	.00428	24.453	.00101	.00586	28.599
75	.00069	.00428	36.652	.00123	.00586	34.148
100	.00087	.00428	45.751	.00141	.00586	38.692
-7	.00010	.00428	5.598	.00063	.00586	18.098
-22	.00001	.00428	-.0165	.00052	.00586	15.124

TABLE 36 - FREQUENCY SCAN OUTPUT DATA FOR SYSTEM B (34.45 & 27.72 Hz)

	f_e=34.45 Hz			f_e=27.72 Hz		
T,°C	R	X	G	R	X	G
25	.00141	-.0024	182.99	.00179	-.0034	120.21
75	.00158	-.0024	192.87	.00195	-.0034	125.62
100	.00177	-.0024	200.36	.00213	-.0034	131.27
-7	.00099	-.0024	147.72	.00133	-.0034	98.93
-22	.00088	-.0024	135.43	.00122	-.0034	92.71

The following observations are made of Tables 35 and 36:

1. SSR resistance and conductance increase and decrease with temperature (undefined at -22°C in mode 1).

2. SSR reactance remains constant for any temperature variation.

The undamping and net damping comparisons for System B are presented in Tables 37 and 38.

TABLE 37 - MAXIMUM UNDAMPING AND NET DAMPING COMPARISON SYSTEM B (MODES 1 & 2)

	Mode 1 (σ_1=0.05) f_e=44.29 Hz X_c=90%			Mode 2 (σ_2=0.113) f_e=39.79 Hz X_c=70%		
T,°C	$\Delta\sigma_1$(max)	σ_{NET}	% Dec.	$\Delta\sigma_2$(max)	σ_{NET}	% Dec.
25	0.3578	-0.3078	-	0.0284	0.0846	-
75	0.5362	-0.4862	58.0	0.0339	0.0791	6.5
100	0.6693	-0.6193	101.2	0.0384	0.0746	11.8
-7	0.0819	-0.0319	-	0.0180	0.0950	-
-22	-.0024	0.0524	-	0.0150	0.0980	-

TABLE 38 - MAXIMUM UNDAMPING AND NET DAMPING COMPARISON SYSTEM B (MODES 3 & 4)

	Mode 3 (σ_3=0.028) f_e=34.45 Hz X_c=60%			Mode 4 (σ_4=0.028) f_e=27.72 Hz X_c=40%		
T,°C	$\Delta\sigma_3$(max)	σ_{NET}	% Dec.	$\Delta\sigma_4$(max)	σ_{NET}	% Dec.
25	0.4996	-0.4716	-	0.3690	-0.3410	-
75	0.5265	-0.4985	5.7	0.3856	-0.3577	4.9
100	0.5470	-0.5190	10.0	0.4030	-0.3750	10.0
-7	0.4033	-0.3753	-	0.3037	-0.2757	-
-22	0.3697	-0.3417	-	0.2846	-0.2566	-

Table 37 shows that, in System B, there can be a decrease of over 100 percent in the net system damping when considerations are made for temperature and frequency. It is also seen that the net damping decreases for all four modes when the system resistances are increased. This can be attributed to the fact that the values of SSR resistance are less than the corresponding SSR reactances. When this is the case, from Equation 2, G_n = SSR R/(SSR R^2 + SSR X^2) implies that, for constant X, an increase in R leads to an increase in G_n. This leads to an increase in the amount of undamping and a decrease in the net damping.

The output data for the cases of System C (maximum conductance values) are shown in Tables 39 & 40.

TABLE 39 - FREQUENCY SCAN OUTPUT DATA
FOR SYSTEM C (35.35 & 27.6 Hz)

	f_e=35.35 Hz			f_e=27.6 Hz		
T,°C	R	X	G	R	X	G
25	.02551	.02256	21.998	.02134	.02275	21.930
75	.02663	.02411	20.636	.02194	.02380	20.938
100	.02760	.02563	19.452	.02257	.02504	19.858
-7	.02247	.01907	25.864	.01899	.01943	25.773
-22	.02157	.01820	27.077	.01829	.01861	26.858

TABLE 40 - FREQUENCY SCAN OUTPUT DATA
FOR SYSTEM C (8.9 Hz)
f_e=8.9 Hz

T,°C	R	X	G
25	.01372	.02357	18.451
75	.01417	.02330	19.050
100	.01499	.02278	20.159
-7	.01114	.02492	14.953
-22	.01054	.02518	14.137

The following observations are made of Tables 39 and 40:

1. The SSR resistance increases and decreases with temperature for all three modes.

2. The SSR reactance increases and decreases with temperature for the first two modes.

3. The SSR reactance increases for a decrease in temperature in the third mode.

4. The SSR conductance increases for a decrease in temperature in the first two modes.

5. The SSR conductance follows temperature in the third mode.

The undamping and net damping comparison for System C is presented in Tables 41 and 42.

TABLE 41 - MAXIMUM UNDAMPING AND NET DAMPING COMPARISON SYSTEM C (MODES 1 & 2)

	Mode 1 (σ_1=0.05) f_e=35.35 Hz X_c=50%			Mode 2 (σ_2=0.05) f_e=27.61 Hz X_c=30%		
T,°C	$\Delta\sigma_1$(max)	σ_{NET}	% Dec.	$\Delta\sigma_2$(max)	σ_{NET}	% Dec.
25	0.4253	-0.3753	-	0.0413	0.0087	-
75	0.3983	-0.3483	-	0.0394	0.0106	-
100	0.3754	-0.3254	-	0.0373	0.0127	-
-7	0.4992	-0.4492	19.7	0.0484	0.0016	81.3
-22	0.5226	-0.4726	25.9	0.0505	-0.0005	105.7

TABLE 42- MAXIMUM UNDAMPING AND NET DAMPING COMPARISON
SYSTEM C (MODE 3)
Mode 3 (σ_3=0.05)

f_e=8.9 Hz

X_c=10%

T,°C	$\Delta\sigma_3$(max)	σ_{NET}	%Decrease
25	0.0431	0.0069	-
75	0.0444	0.0056	18.8
100	0.0470	0.0030	56.5
-7	0.0348	0.0152	-
-22	0.0329	0.0171	-

For modes 1 and 2 in System C, the net damping decreases with temperature (and resistance), whereas for mode 3 the net damping decreases with increased temperature. For System C, the decrease in damping was largest for mode 2, with a decrease in net damping of over 105 percent for a conductor temperature of -22°C. In addition, this case represents a change from stable to unstable conditions for the generator in System C, as the net damping goes from positive to negative.

The output data for the GEN1 study of System D (maximum conductance values) are shown in Tables 43 and 44.

TABLE 43 - FREQUENCY SCAN OUTPUT DATA FOR SYSTEM D
GEN1 (35.35 & 27.6 Hz)

	f_e=35.35 Hz			f_e=27.6 Hz		
T,°C	R	X	G	R	X	G
25	.01388	.01262	39.452	.03246	-.0084	28.889
75	.01495	.01315	37.714	.03372	-.0067	28.550
100	.01598	.01372	36.030	.03510	-.0045	28.027
-7	.01142	.01155	43.276	.02793	-.0133	29.153
-22	.01078	.01131	44.144	.02667	-.0145	28.977

TABLE 44 - FREQUENCY SCAN OUTPUT DATA
FOR SYSTEM D GEN1 (8.9 Hz)

f_e=8.9 Hz

T,°C	R	X	G
25	.00692	.02483	10.412
75	.00696	.02469	10.585
100	.00704	.02441	10.905
-7	.00656	.02561	9.386
-22	.00646	.02578	9.145

The following observations are made of Tables 43 and 44:

1. The SSR resistance increases and decreases with temperature for all three modes.
2. The SSR reactance increases and decreases with temperature for the first two modes.
3. The SSR reactance increases for a decrease in temperature in the third mode.
4. The SSR conductance increases for a decrease in temperature in the first two modes (-22°C, mode 2 undefined).
5. The SSR conductance follows temperature in the third mode.

The output data for the GEN2 study of System D (maximum conductance values) are shown in Table 45.

TABLE 45 - FREQUENCY SCAN OUTPUT DATA FOR SYSTEM D GEN2 (35.35 & 15.01 Hz)

	f_e=35.35 Hz			f_e=15.01 Hz		
T,°C	R	X	G	R	X	G
25	.01978	.02341	21.054	.00648	.02098	13.437
75	.02099	.02456	20.109	.00664	.02120	13.454
100	.02211	.02575	19.196	.00690	.02158	13.441
-7	.01675	.02105	23.151	.00557	.02000	12.918
-22	.01591	.02050	23.634	.00533	.01980	12.679

The following observations are made of Table 45:

1. The SSR resistance and reactance increase and decrease with temperature for both modes.

2. The SSR conductance increases for a decrease in temperature in the first mode.

3. The SSR conductance follows temperature in the second mode (100°C undefined).

The undamping and net damping comparison for System D is presented in Tables 46 through 48. This system contains two different generators (GEN1 & GEN2), and comparisons of the data for each generator is presented.

TABLE 46 - MAXIMUM UNDAMPING AND NET DAMPING COMPARISON SYSTEM D - GEN1 (MODES 1 & 2)

	Mode 1 (σ_1=0.05) f_e=35.35 Hz X_c=70%			Mode 2 (σ_2=0.05) f_e=27.61 Hz X_c=50%		
T,°C	$\Delta\sigma_1$(max)	σ_{NET}	% Dec.	$\Delta\sigma_2$(max)	σ_{NET}	% Dec.
25	0.7627	-0.7127	-	0.0544	-0.0044	-
75	0.7279	-0.6779	-	0.0537	-0.0037	-
100	0.6954	-0.6454	-	0.0527	-0.0027	-
-7	0.8352	-0.7852	10.2	0.0548	-0.0048	9.1
-22	0.8520	-0.8020	12.5	0.0545	-0.0045	2.3

TABLE 47 - MAXIMUM UNDAMPING AND NET DAMPING COMPARISON
SYSTEM D - GEN1 (MODE 3)
Mode 3 (σ_3=0.05)

f_e=8.9 Hz

X_c=10%

T,°C	$\Delta\sigma_3$(max)	σ_{NET}	%Decrease
25	0.0243	0.0257	-
75	0.0247	0.0253	1.6
100	0.0254	0.0246	4.3
-7	0.0219	0.0281	-
-22	0.0213	0.0287	-

TABLE 48 - MAXIMUM UNDAMPING AND NET DAMPING COMPARISON
SYSTEM D - GEN2 (MODES 1 & 2)

	Mode 1 (σ_1=0.025) f_e=35.35 Hz X_c=70%			Mode 2 (σ_2=0.025) f_e=15.01 Hz X_c=10%		
T,°C	$\Delta\sigma_1$(max)	σ_{NET}	% Dec.	$\Delta\sigma_2$(max)	σ_{NET}	% Dec.
25	0.2159	-0.1909	-	0.0009	0.0241	-
75	0.2063	-0.1813	-	0.0009	0.0241	-
100	0.1969	-0.1719	-	0.0008	0.0242	-
-7	0.2375	-0.2125	11.3	0.0008	0.0242	-
-22	0.2424	-0.2174	13.9	0.0008	0.0242	-

System D produced the same patterns for both generators as System C. Thus it can be stated for these systems that, for lower torsional modes (f_n less than 35 hertz), a decrease in transmission system resistances will generally be accompanied by a decrease in the net system damping. Further, for increases in the system resistances, there will be a corresponding decrease in the net damping for the higher machine torsional modes (f_n greater than 50 hertz).

Inspection of the output data for all the cases in this study reveals that electrical system resonance never occurs (SSR reactance does not equal zero) at the study frequencies. Definite patterns in output data were established for the study systems, with few discrepancies. It was seen that undamping is dependent upon the electrical frequencies and the electrical system configuration (series or parallel impedances).

Conclusions

The results of this study indicate that, under certain temperature extremes and system operating conditions, the amount of undamping present in a system will increase appreciably beyond the undamping which is calculated for transmission system resistances based upon 25°C and 60 Hz. The net system damping was seen to decrease by over 100 percent in several cases, and in one case the net damping became negative, while the base case damping was still positive. The following observations may be drawn from the data contained in the tables in this chapter:

1. For System A, the results obtained in this study indicate that the net system damping may decrease for both increased and decreased conductor resistances.

2. For System B, increased conductor operating temperatures resulted in decreased net system damping. The problem becomes more severe as the conductor temperature and the corresponding resistance increased.

3. For Systems C and D, a decrease in conductor temperature was accompanied by a decrease in the net system damping for torsional modal frequencies that were less than approximately 35 Hz, whereas increased conductor temperature led to a decrease in the net damping for torsional modes greater than approximately 50 Hz.

It was also noted that the system which contained only series impedances demonstrated a constant SSR reactance at a constant frequency when resistances were varied, as expected. For systems containing parallel impedances, a change in resistances resulted in branch impedances changes, and a corresponding change in the value of the parallel impedance. The SSR reactance changed as a result.

To minimize some of the inaccuracies which may occur as a result of differing conductor temperatures and operating frequencies, frequency scan programs should be equipped with the capability to adjust resistances for the appropriate thermal and electrical conditions. Maximum and minimum temperatures which are expected could be included with input data, and the resistances could be adjusted for temperature and frequency while the program is adjusting the reactance values.

Further research in the area of resistance variations in electric power systems and the application to frequency scanning studies is necessary in order further verify these results. One area of interest would be the generator step-up transformer, whose resistance, though more complex than transmission lines, is also dependent upon operating temperatures and frequency. Another area which can be further researched is the equivalent system impedance which is used to represent adjoining systems, be they loads or bulk transmission grids. Finally, the generator itself is another area which may also be studied, as the stator and rotor resistances are influenced strongly by frequency.

APPENDIX A

STUDY SYSTEM BASE CASES

There are four different systems which will be studied. Two are representative of actual transmission networks in eastern and northern Arizona. All four systems have been studied previously in great detail.

Coronado System

The Coronado system (System A) includes many of the extra-high voltage (EHV) transmission lines in eastern Arizona. The single line diagram of System A is shown in Figure 1. Extensive studies by Salt River Project (SRP) have indicated that the System A configuration can lead to severe torsional interaction problems. Coronado is tied radially to the Cholla Generating Station via one seventy three mile, 500 kV line. The conductor is 2156 ACSR, single circuit, with two conductors per bundled phase. Two other major transmission lines from Coronado are assumed to be out of service. A reactor is shown at the Coronado end of the Coronado to Cholla line, and there is series compensation on four major lines emanating from Cholla. The series compensation in each of these four transmission lines is varied during frequency scanning studies to obtain a variety of system resonant conditions.

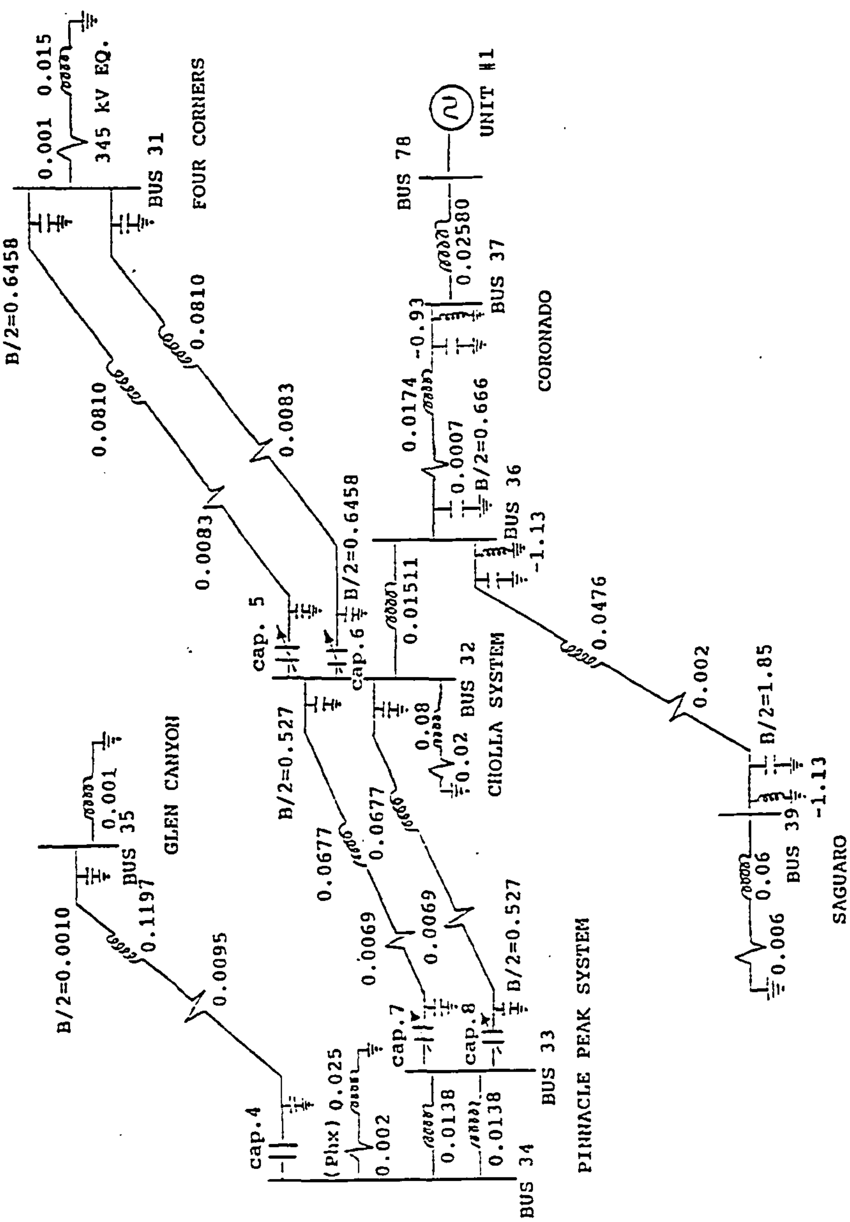

FIGURE 1 - CORONADO SYSTEM (SYSTEM A)

There are two turbine-generators at Coronado Generating Station, which is located near St. Johns in eastern Arizona. Each generating unit is rated at 456.6 MVA, but only one unit is on-line for this study. The modal frequencies for the Coronado generators and the corresponding values of modal inertia and no load damping are shown in Table 49. All values are on a 100 MVA base.

TABLE 49 - CORONADO MODAL MECHANICAL SPRING MASS MODEL DATA

Mode	H_n	f_n	σ_n (No Load)
1	20.44	33.88	0.042
2	44.68	44.61	0.029

The Coronado induction generator data which is used in frequency scanning studies was evaluated by SRP from information supplied by General Electric and is shown in Table 50. The input data listing for System A is shown in Figure 2. Frequency scan output plots for the levels of compensation which resulted in maximum undamping values (transmission system resistances based on 25°C, 60 Hz) for modes 1 and 2 of the Coronado generator are shown in Figures 3 and 4, respectively.

TABLE 50 - CORONADO GENERATOR DATA

p.u Slip	$R_{p.u.}$	$X_{p.u.}$
0.166667	0.0205000	0.1645760
0.333333	0.0104700	0.1250000
0.500000	0.0045000	0.0912500
0.666667	0.0005000	0.0601600
0.833333	-0.002330	0.0300000
1.000000	-0.004500	0.0000000

```
COR #1 SSR UNDAMPING TEST (SYSTEM A)
               211  11
      50.0        5.00        10.0
      26.6        15.3
 01
 02
 03
 04
 05
 06
 07
 08
 09
 10
 11
 12
 13
 14
 15
    4           36.00                      GLC-SYS R-L-C EQ COMP
    5           50.00                      FCN-CHO LINE COMP(CHO)#1
    6           50.00                      FCN-CHO LINE COMP(CHO)#2
    7           40.00                      CHO-PPK LINE COMP(PPK)#1
    8           40.00                      CHO-PPK LINE COMP(PPK)#2
  999
    5.0001.0001.0001.000112.5025.0025.0025.0025.0025.0025.00
    6.0001.0001.0001.000112.5025.0037.5037.5037.5037.5037.50
    7.000116.0032.0040.0040.0040.0016.0024.0024.0032.0040.00
    8.000116.0032.0040.0040.0040.0016.0024.0040.0032.0040.00
  999
         1      4.566          CORONADO UNITS 1,2 OR 3
0.1666666 0.0205000 0.1645760
0.3333333 0.0104700 0.1250000
0.5000000 0.0045000 0.0912500
0.6666666 0.0005000 0.0601600
0.8333333 -.0023300 0.0300000
 1.0000000 -.0045000 0.0000000

         999
  19 31 32                   5  .6458   .0083     .0810     1.030 FCN-CHO 345 #1
  20 31 32                   6  .6458   .0083     .0810     1.030 FCN-CHO 345 #2
  21 32 33                   7 0.5270   .0069     .0677     1.030 CHO-PPK 345 #1
  22 32 33                   8 0.5270   .0069     .0677     1.030 CHO-PPK 345 #2
  23 34 35          4          0.0010   .0095     .1197     1.020 GLC-SYS R-L-C
  24 36 37          -0.930     0.6660   .0007     .0174     1.060 CHO-COR 500KV
  39 36 39-1.130    -1.130     1.8500   .0020     .0476     1.060 CHO-SAG 500KV
 999
  42 37 78                      0.02580   1.070 COR UNIT 1 TRANSFORMER
  45 78  0 1 1                            1.070 COR UNIT 1
  48 36 32                      0.01511   1.060 CHO 500/345KV #1
  65 33 34                      0.01380   1.080 PPK 345/230KV #1
  66 33 34                      0.01380   1.080 PPK 345/230KV #2
  86 35  0                      0.00100   1.020 GLC 345KV BUS FOR R-L-C EQ
  73 31  0           0.00100    0.01500   1.030 FC 345KV EQ FOR 230KV
  70 34  0           0.00200    0.02500   1.000 PPK 230KV EQ FOR PHX SYS
  85 32  0           0.02000    0.08000   1.030 CHO 345KV EQ FOR 230KV SYS
  94 39  0           0.00600    0.06000   1.050 SAG 500KV EQ
 999
   78    1
CORONADO (SYSTEM A)

DUMMY
  999
```

FIGURE 2 - SYSTEM A INPUT DATA LISTING

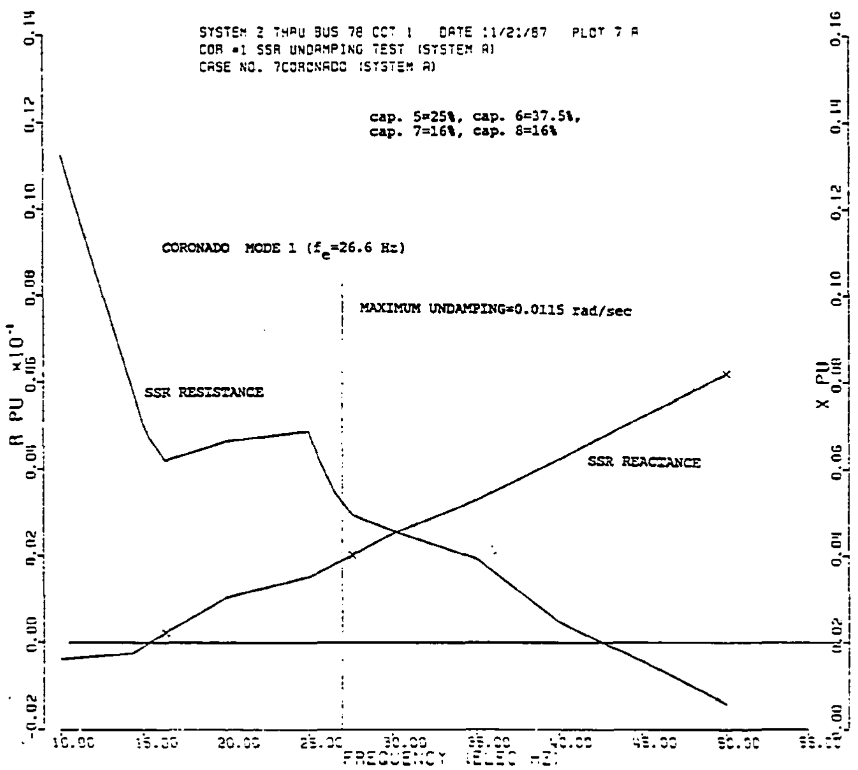

FIGURE 3 - SYSTEM A FREQUENCY SCAN OUTPUT PLOT - MAXIMUM UNDAMPING IN MODE 1

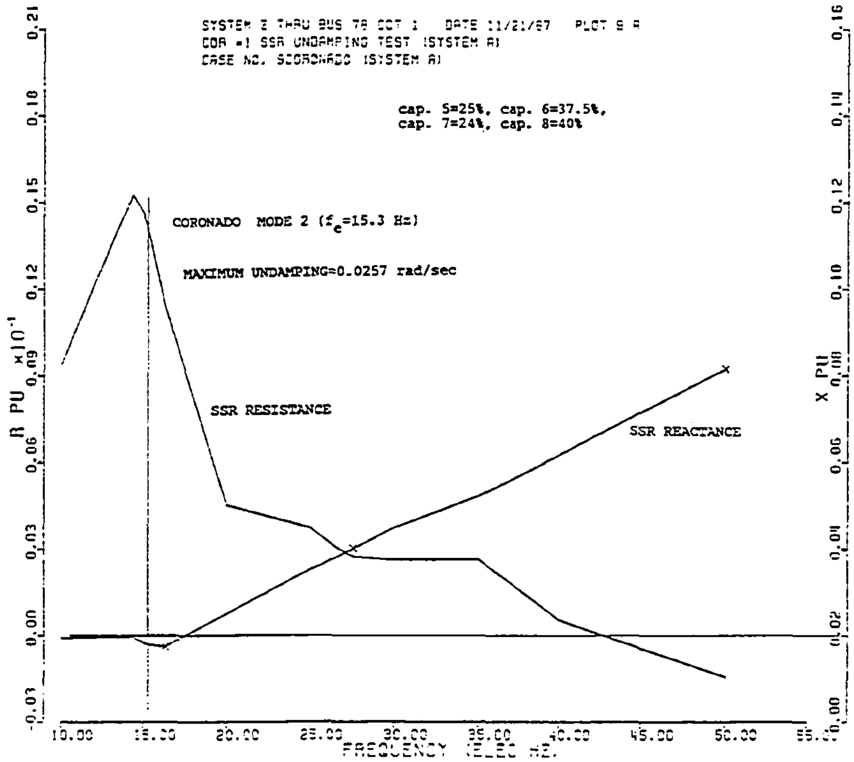

FIGURE 4 - SYSTEM A FREQUENCY SCAN OUTPUT PLOT -
MAXIMUM UNDAMPING IN MODE 2

Series Resonance System

The series resonance system (System B) was proposed in an IEEE paper entitled "First Benchmark Model for Computer Simulation of Subsynchronous Resonance" (1977), and uses a portion of the Navajo 500 kV transmission system. A single line diagram depicting the Navajo Generating Station, which is located in northern Arizona, and a radial tie to a remote transmission facility is shown in Figure 5. For this system configuration involving the Navajo system, two other major transmission lines are assumed to be out of service.

The Navajo to McCullough line is 274 miles long and is composed of 2156 ACSR conductor, single circuit, with two conductors per bundled phase. The series compensation in this line is generally about 70 percent. For this study, the series compensation in the system, (X_c), was varied from 0 percent to 90 percent of the inductive reactance in the Navajo to McCullough line.

Only one of the three Navajo units, each of which is rated about 890 MVA, is connected to the electrical network for this study. Values for the modal inertia, modal frequency and machine damping at no load for the modal frequencies of each of the Navajo generators are shown in Table 51.

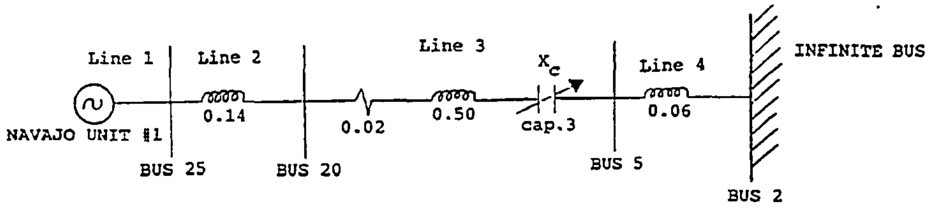

FIGURE 5 - SERIES RESONANCE SYSTEM (SYSTEM B)

TABLE 51 - NAVAJO MODAL MECHANICAL SPRING MASS MODEL DATA

Mode	H_n	f_n	σ_n (No Load)
1	2.70	15.71	0.050
2	27.80	20.21	0.113
3	6.92	25.55	0.028
4	3.92	32.28	0.028

The induction generator data for the Navajo unit was made available in an IEEE paper (Agrawal and Farmer, 1979). This data is reproduced in Table 52.

TABLE 52 - NAVAJO GENERATOR DATA

p.u. Slip $\frac{(60-f)}{60}$	Manufacturer-Supplied Impedance		Adjusted Impedance For SSR Studies	
	$R_{p.u.}$	$X_{p.u.}$	$R_{p.u.}$	$X_{p.u.}$
.1667	.0337	.1815	.0246	.1515
.3333	.0220	.1747	.0112	.1165
.5000	.0172	.1713	.0051	.0857
.6667	.0147	.1692	.0012	.0564
.8333	.0132	.1680	-.0013	.0280
1.0000	.0122	.1671	-.0035	.0000

The adjusted impedances for corresponding slip values are shown. The manufacturer-supplied impedance data for the G.E. generator are based upon 60 Hz stator frequency and variable rotor speed, and were adjusted by Agrawal and Farmer to represent variable stator frequency and fixed rotor speed.

The transmission line impedance values which were presented in the First Benchmark Model paper are based on 892.4 MVA, 500 kV. The frequency scan program SRPRES requires that impedance values be on a 100 MVA, 500 kV base. A base change in the per unit quantities was made (all impedances were multiplied by 100/892.4). The input data listing for System B is shown in Figure 6. The frequency scan output data obtained correlates fairly well with the data obtained by Agrawal and Farmer, and any differences can easily be explained by roundoff in translation.

Frequency scan output plots for the levels of compensation which resulted in maximum undamping values for each of the four torsional modes of the Navajo generator (transmission system resistances based on 25°C, 60 Hz) are shown in Figures 7 through 10.

```
SERIES RESONANCE CASE-FIRST BENCHMARK MODEL
                211  11
     50.0       5.00      10.0
    44.29      39.79     34.45     27.72
 01
 02
 03
 04
 05
 06
 07
 08
 09
 10
 11
 12
 13
 14
 15
   3          36.00                    XC-CAPACITOR BETWEEN A B
  999
   3.000120.0040.0060.0070.0090.00
  999
        1      8.924          NAVAJO UNIT 1
0.1666666 0.0246000 0.1515000
0.3333333 0.0112000 0.1165000
0.5000000 0.0051000 0.0857000
0.6666666 0.0012000 0.0564000
0.8333333 -.0013000 0.0280000
1.0000000 -.0035000 0.0000000

       999
  3  5 20                    3  .00001  0.0022410 0.0560290 1.000 LINE #3
 999
  5  2  0            0.00001  0.00001   1.000 INFINITE BUS REPRESENTATION
  4  2  5                     0.00672   1.000 LINE #4
  2 20 25                     0.01569   1.000 NAV UNIT 1 S.U.TRANSFORMER
  1 25  0 1 1                           1.000 NAV UNIT 1
 999
  25    1
SERIES RESONANCE (SYSTEM B)

DUMMY
  999
```

FIGURE 6 - SYSTEM B INPUT DATA LISTING

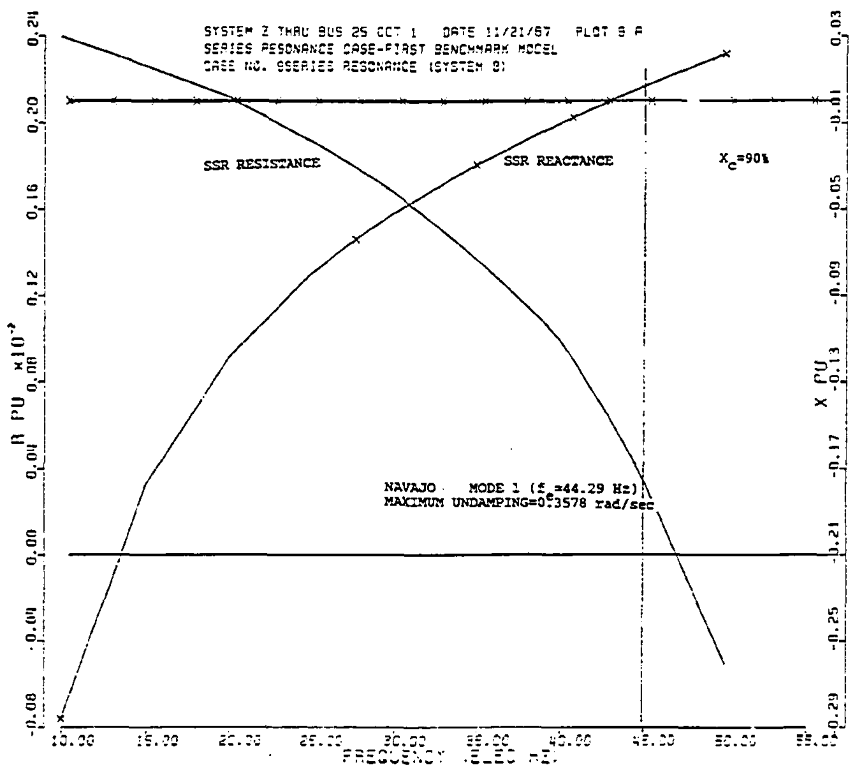

FIGURE 7 - SYSTEM B FREQUENCY SCAN OUTPUT PLOT - MAXIMUM UNDAMPING IN MODE 1

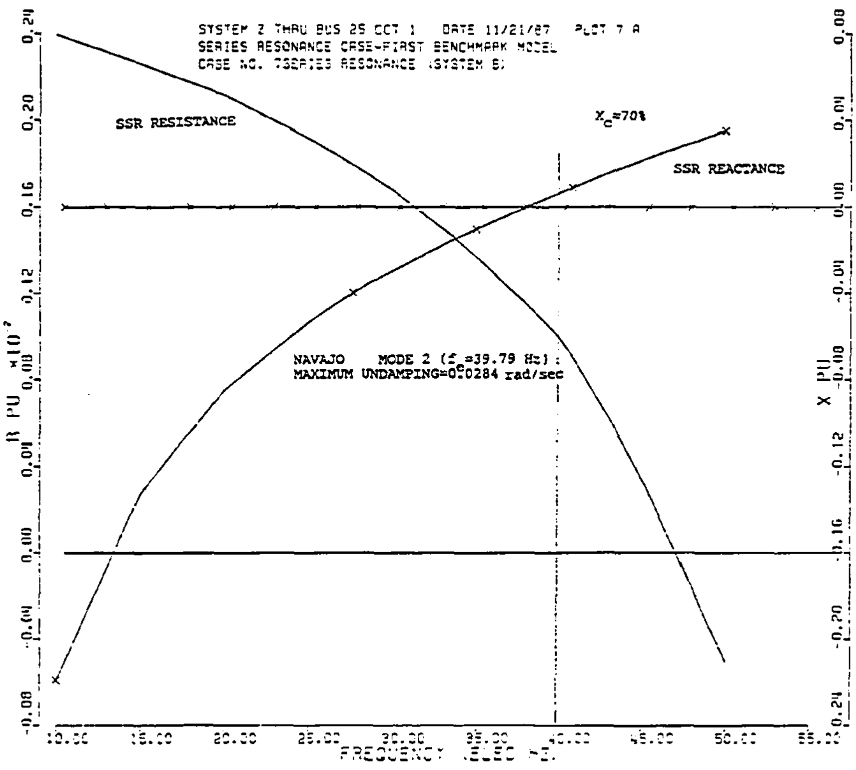

FIGURE 8 - SYSTEM B FREQUENCY SCAN OUTPUT PLOT -
MAXIMUM UNDAMPING IN MODE 2

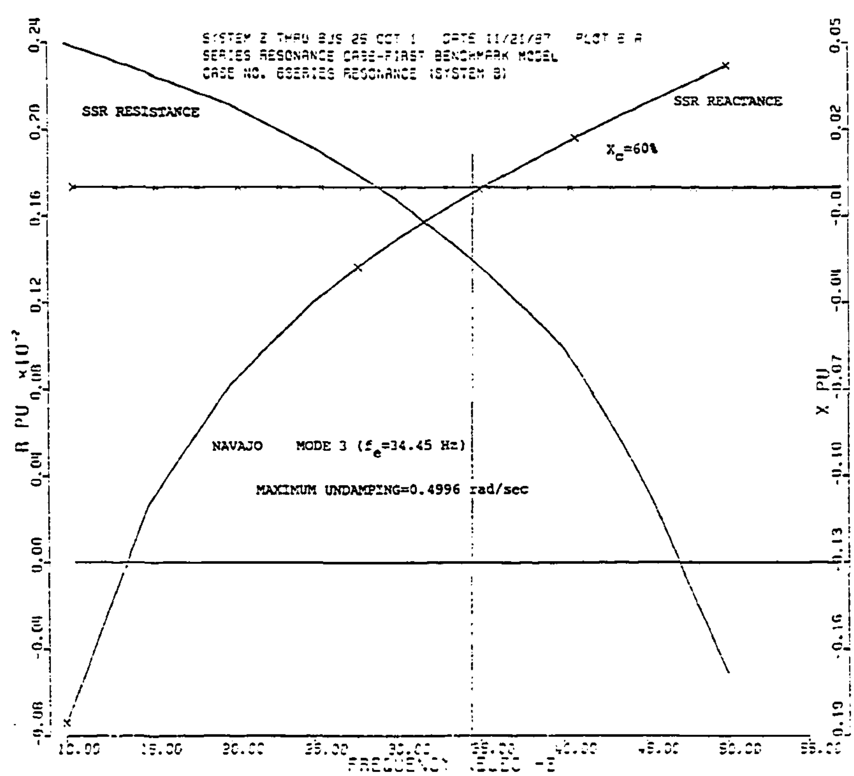

FIGURE 9 - SYSTEM B FREQUENCY SCAN OUTPUT PLOT - MAXIMUM UNDAMPING IN MODE 3

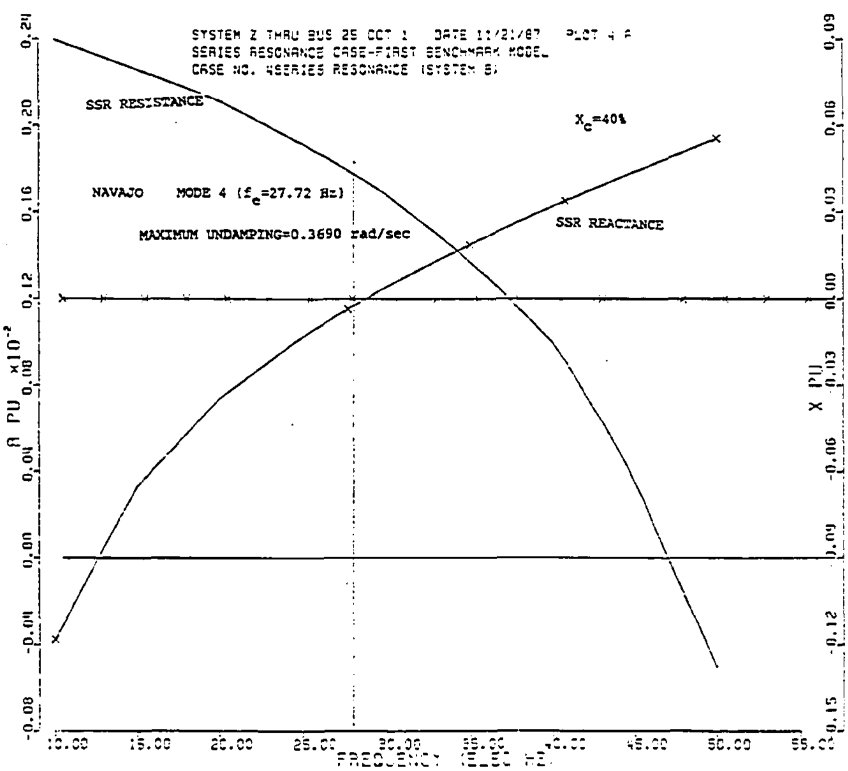

FIGURE 10 - SYSTEM B FREQUENCY SCAN OUTPUT PLOT - MAXIMUM UNDAMPING IN MODE 4

Parallel Resonance Systems

There are two different parallel resonance systems to be analyzed in this part of the study, both of which were presented by the IEEE Subsynchronous Resonance Working Group in a paper entitled "Second Benchmark Model for Computer Simulation of Subsynchronous Resonance" (1985). These systems are shown in Figure 11 (System C) and Figure 12 (System D). Each system has one series capacitor, with compensation levels which vary from ten to ninety percent of the line reactance.

The generator in System C (GEN1) is rated 6 MVA. Two generators are studied in System D, each of which has different MVA ratings and step-up transformer impedances. The first generator in System D is the same as the generator in System C. The second generator in System D (GEN2) is rated 7 MVA. The torsional modal frequencies for GEN1 and GEN2 and the corresponding values for inertia and no load damping are shown in Table 53. The induction generator data for each generator was presented in the Second Benchmark paper and is reproduced in Tables 54 and 55.

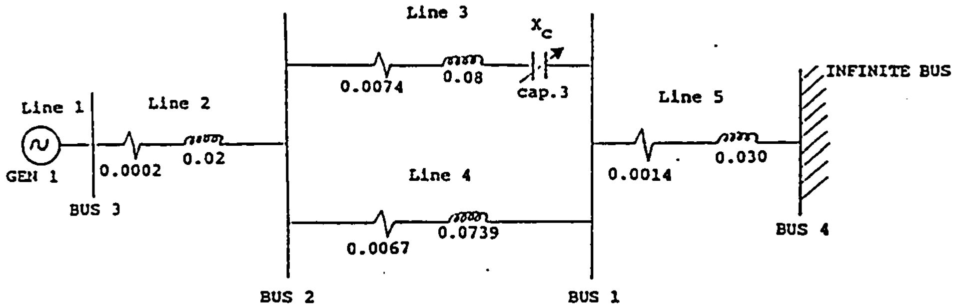

FIGURE 11 - PARALLEL RESONANCE SYSTEM (SYSTEM C)

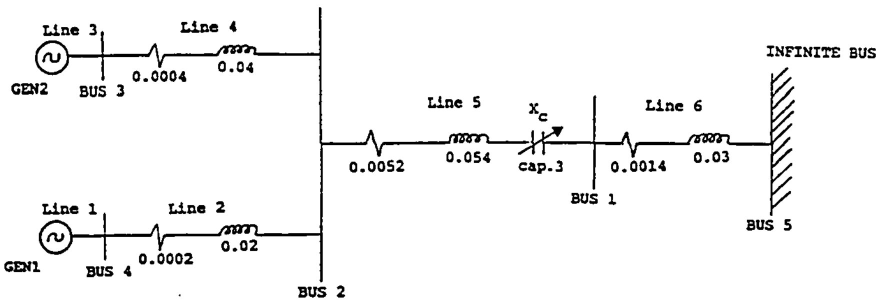

FIGURE 12 - PARALLEL RESONANCE SYSTEM (SYSTEM D)

TABLE 53 - GEN1, GEN2 MODAL MECHANICAL SPRING MASS MODEL DATA

	GEN1			GEN2		
Mode	f_n	H_n	σ_n(NL)	f_n	H_n	σ_n(NL)
1	24.65	1.55	0.050	24.65	2.495	0.025
2	32.39	9.39	0.050	44.99	93.960	0.025
3	51.10	74.80	0.050			

TABLE 54 - GEN1 GENERATOR DATA

p.u. Slip $\frac{(60-f)}{60}$	Impedance	
	$R_{p.u.}$	$X_{p.u.}$
.1667	.0223	.1716
.3333	.0067	.1344
.5000	.0012	.1004
.6667	-.0017	.0668
.8333	-.0034	.0334

TABLE 55 - GEN2 GENERATOR DATA

p.u. Slip $\frac{(60-f)}{60}$	Impedance	
	$R_{p.u.}$	$X_{p.u.}$
.1667	.0288	.1576
.3333	.0096	.1217
.5000	.0026	.0906
.6667	-.0009	.0602
.8333	-.0031	.0301

The generator resistances given in the IEEE paper must be multiplied by -1 before they can be used by SRPRES. This is because the resistance values supplied by the manufacturer are assumed to be negative by most frequency scanning programs and are thus automatically assigned a negative sign. This is not the case, however, with SRPRES. The input data listings for System C and System D are shown in Figures 13 and 14, respectively.

```
PARALLEL RESONANCE SYSTEM(SYS1)-SECOND BENCHMARK MODEL
             211  11
     50.0        5.00       5.0
     35.35      27.61       8.90
 01
 02
 03
 04
 05
 06
 07
 08
 09
 10
 11
 12
 13
 14
 15
    3     36.00                        LINE #3 COMPENSATION
  999
    310.0020.0030.0040.0050.0060.0070.0080.0090.00
  999
          1   6.000            SYS1 UNIT 1
0.1666666 0.0223000 0.1716000
0.3333333 0.0067000 0.1344000
0.5000000 0.0012000 0.1004000
0.6666666 -.0017000 0.0668000
0.8333333 -.0034000 0.0334000

       999
   3  1  2          3          0.00001    0.00740    0.08000    1.000 LINE #3
 999
   6  4  0           0.00001    0.00001    1.000 INFINITE BUS
   2  2  3           0.0002     0.02000    1.000 SYS1 STEP-UP TRANSFORMER
   1  3  0 1 1                             1.000 SYS1 GENERATOR
   4  1  2           0.0067     0.07390    1.000 LINE #4
   5  4  1           0.0014     0.03000    1.000 LINE #5
 999
    3    1
PARALLEL RESONANCE (SYSTEM C)

DUMMY
  999
```

FIGURE 13 - SYSTEM C INPUT DATA LISTING

```
PARALLEL RESONANCE SYSTEM(SYS2)-SECOND BENCHMARK MODEL
              211  11
    50.0         5.00       5.0
    35.35       15.01
 01
 02
 03
 04
 05
 06
 07
 08
 09
 10
 11
 12
 13
 14
 15
   3     36.00                          LINE #5 COMPENSATION
  999
   310.0020.0030.0040.0050.0060.0070.0080.0090.00
  999
        1   6.000             SYS2 UNIT 1
0.1666666 0.0223000 0.1716000
0.3333333 0.0067000 0.1344000
0.5000000 0.0012000 0.1004000
0.6666666 -.0017000 0.0668000
0.8333333 -.0034000 0.0334000

        2   7.000             SYS2 UNIT 2
0.1666666 0.0288000 0.1576000
0.3333333 0.0096000 0.1217000
0.5000000 0.0026000 0.0906000
0.6666666 -.0009000 0.0602000
0.8333333 -.0031000 0.0301000

      999
  5  1  2         3           0.00001   0.0052    0.05400   1.000 LINE #5
 999
  2  2  4           0.0002    0.02000   1.000 SYS2 GEN1 S.U. TRANSF
  1  4  0 1 1                           1.000 SYS2 GENERATOR #1
  3  3  0 2 1                           1.000 SYS2 GENERATOR #2
  4  2  3           0.0004    0.04000   1.000 SYS2 GEN2 S.U. TRANSF
  6  5  1           0.0014    0.03000   1.000 LINE #6
  7  5  0           0.00001   0.00001   1.000 INFINITE BUS
 999
   3    2
PARALLEL RESONANCE (SYSTEM D)

DUMMY
  999
```

FIGURE 14 - SYSTEM D INPUT DATA LISTING

Frequency scan output plots for the compensation levels in System C which resulted in maximum undamping values for each of the three torsional modes of GEN1 are shown in Figures 15 through 17. For System D, output plots corresponding to maximum undamping values for the three modes of GEN1 are shown in Figures 18 through 20. The plots for the level of compensation which resulted in maximum undamping for the two modes of GEN2 in System D are shown in Figures 21 and 22. These plots are for the cases with transmission system resistances based on 25°C, 60 Hz.

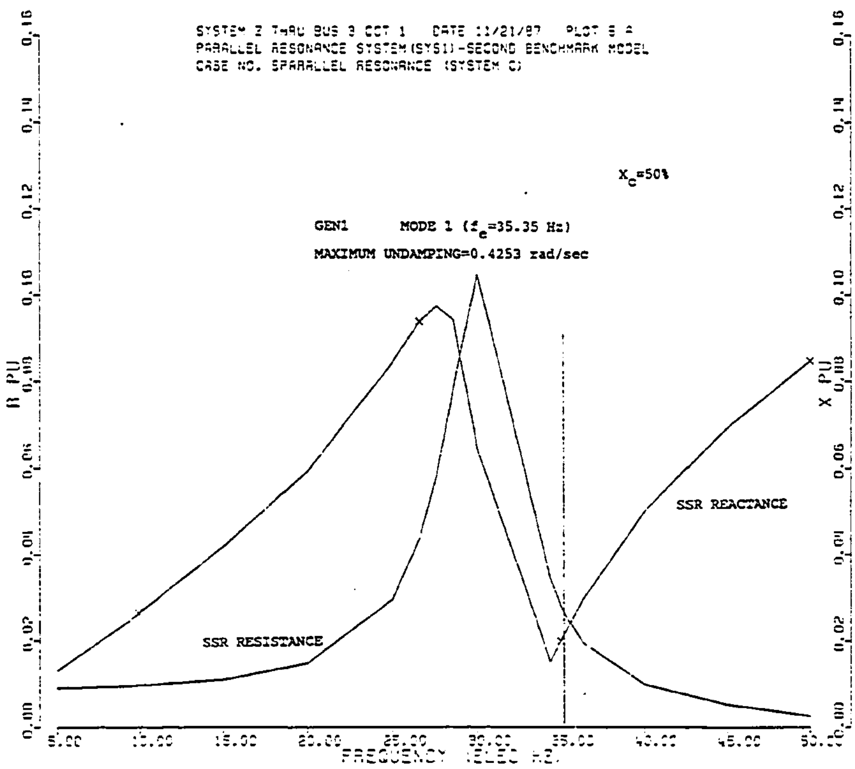

FIGURE 15 - SYSTEM C FREQUENCY SCAN OUTPUT PLOT - MAXIMUM UNDAMPING IN MODE 1

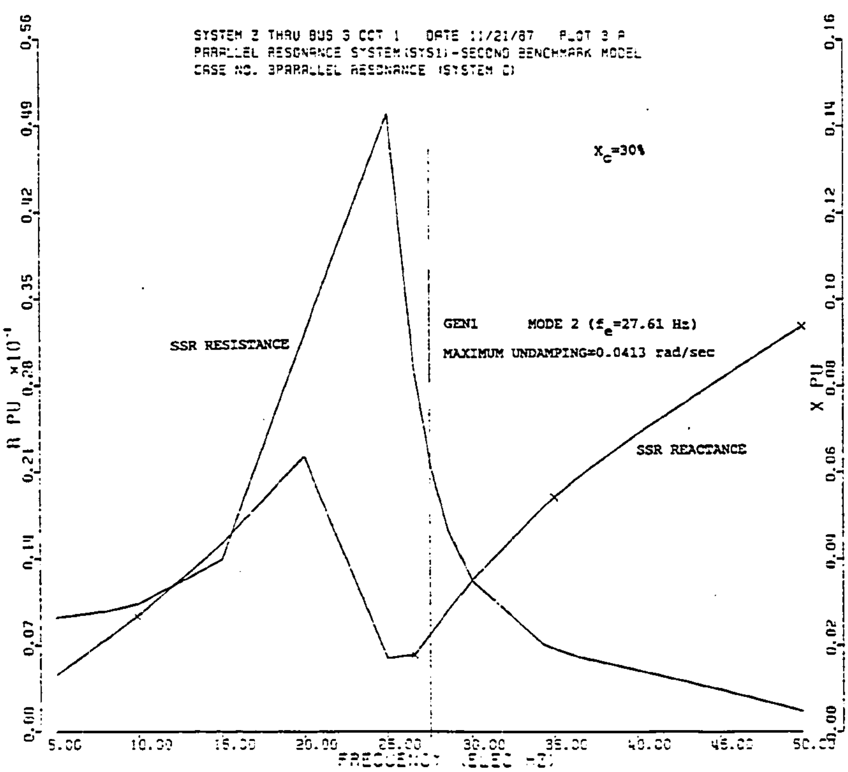

FIGURE 16 - SYSTEM C FREQUENCY SCAN OUTPUT PLOT - MAXIMUM UNDAMPING IN MODE 2

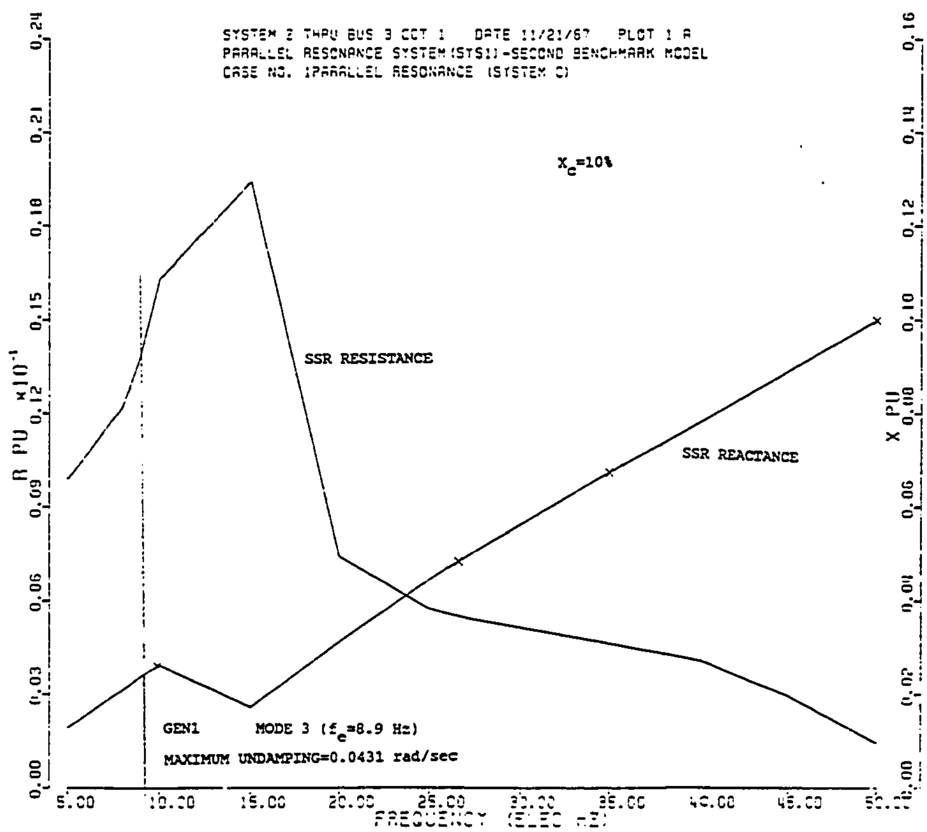

FIGURE 17 - SYSTEM C FREQUENCY SCAN OUTPUT PLOT - MAXIMUM UNDAMPING IN MODE 3

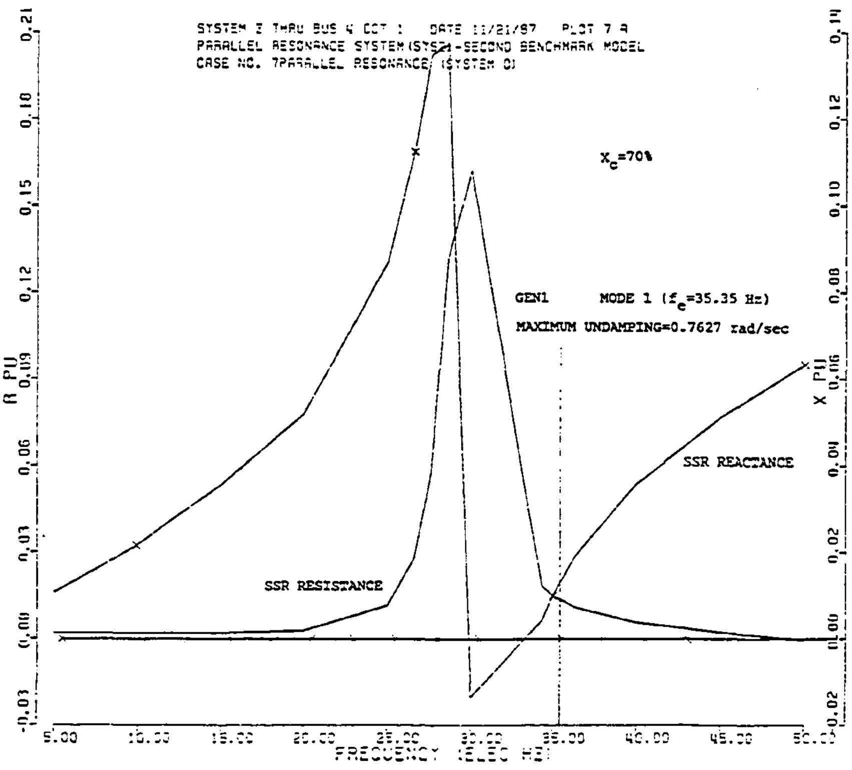

FIGURE 18 - SYSTEM D FREQUENCY SCAN OUTPUT PLOT -
MAXIMUM UNDAMPING IN GEN1 MODE 1

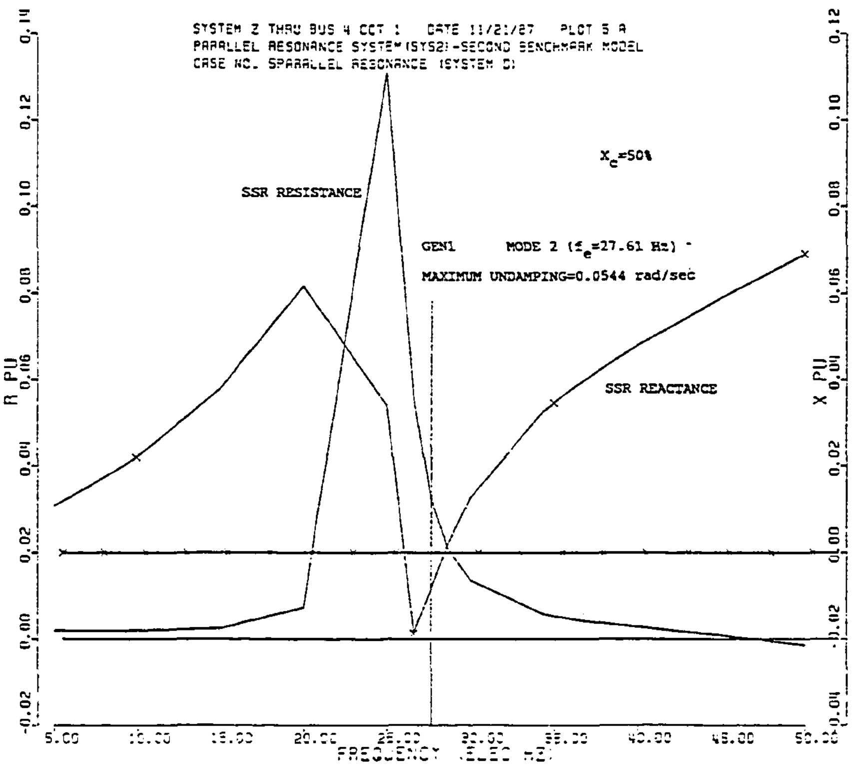

FIGURE 19 - SYSTEM D FREQUENCY SCAN OUTPUT PLOT - MAXIMUM UNDAMPING IN GEN1 MODE 2

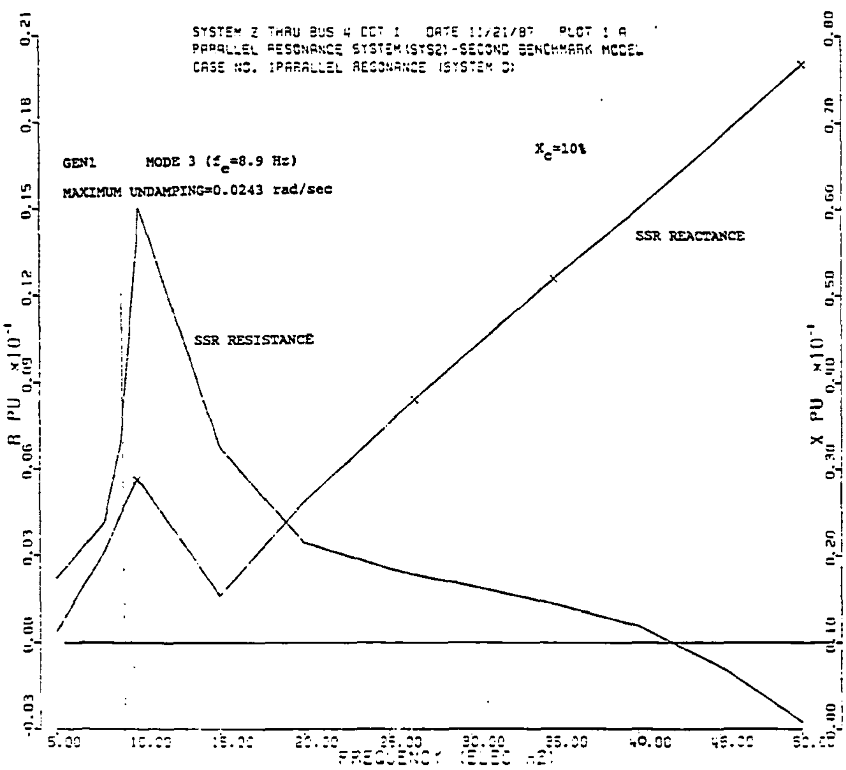

FIGURE 20 - SYSTEM D FREQUENCY SCAN OUTPUT PLOT - MAXIMUM UNDAMPING IN GEN1 MODE 3

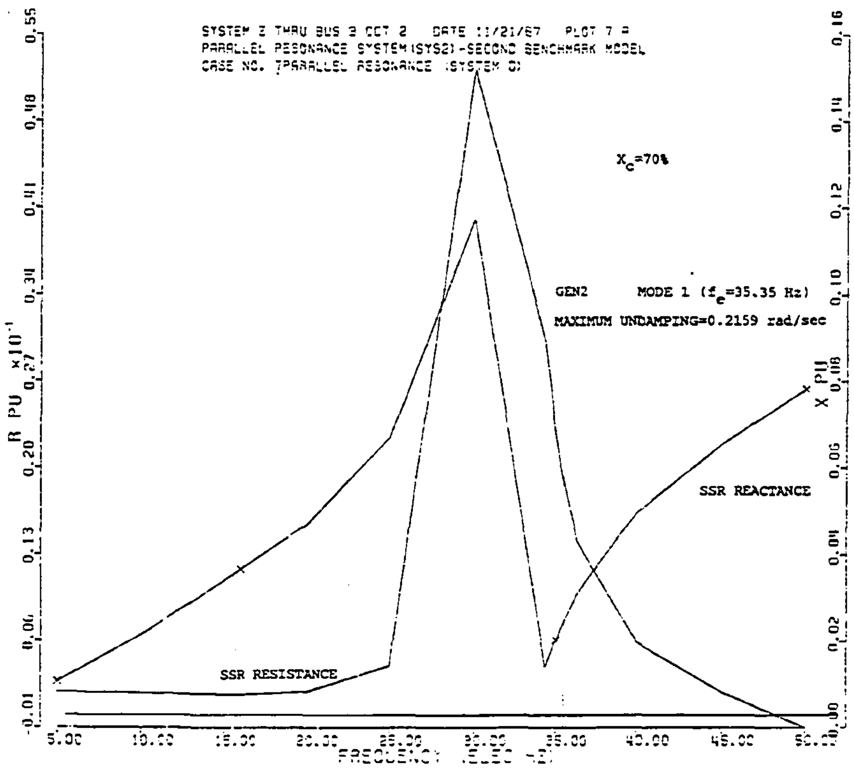

FIGURE 21 - SYSTEM D FREQUENCY SCAN OUTPUT PLOT -
MAXIMUM UNDAMPING IN GEN2 MODE 1

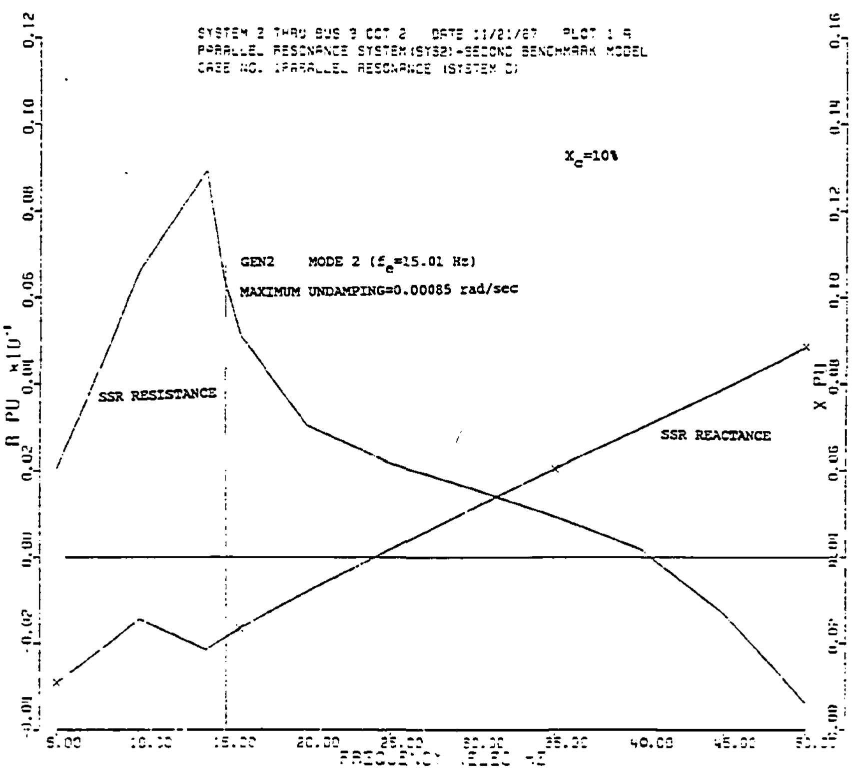

FIGURE 22 - SYSTEM D FREQUENCY SCAN OUTPUT PLOT - MAXIMUM UNDAMPING IN GEN2 MODE 2

APPENDIX B

SRPRES, A FREQUENCY SCANNING PROGRAM

The frequency scanning program is an analytical tool used to identify potential steady state subsynchronous resonance problems at utility generating stations. Basically, the program calculates the driving point impedance for the electric system as viewed from the study bus over a specified range of subsynchronous frequencies. The SSR resistance and reactance values are then plotted as a function of frequency, and possible SSR problems may then be determined by visually inspecting the output plots and data.

The measure of undamping, or negative damping, is determined by visual inspection of the plotted impedances. In the neighborhood of low reactance values, if the SSR resistance is negative, an induction generator problem is indicated. The magnitude of the negative resistance is a measure of the growth rate of electrical oscillations.

The output of SRPRES may also be used to determine if a torsional interaction problem exists. Calculation of specific values for undamping at the modal frequencies are calculated using Equation 1 and the conductance values which are produced as part of the output data from the frequency scan. The value of undamping is compared to the natural machine damping. If the magnitude of undamping exceeds the machine damping, a torsional interaction problem is indicated.

SRPRES Background

SRPRES, the software used by Salt River Project (SRP) for frequency scanning analysis, has the capability to analyze several machines connected to a common bus in addition to different combinations of transmission line outages and ranges of series compensation levels in designated transmission lines. With these features, rapid identification of potentially hazardous network configurations and series compensation levels can be identified.

SRPRES was originally written by General Electric (entitled RESOUT) to identify resonance conditions in electric power systems. Southern California Edison (SCE) then modified the program to permit the calculation of resonance in networks containing transmission loops by using a Z-bus matrix approach. Arizona Public Service (APS) obtained the software from SCE and added a frequency scanning feature. Finally, SRP obtained the program and added various minor program enhancements.

Method of Analysis

The program models the transmission system as a single phase positive sequence branch-node network. At each frequency step, an equivalent pi representation for designated transmission lines is computed, with shorter lines being treated as simple R-L branches, and the Y-BUS matrix of the network is formed. Y-BUS is then inverted by Gaussian elimination to form Z-BUS, and the diagonal element of the Z-BUS matrix corresponding to the generator mode of interest is the driving point impedance. This network driving point impedance is then combined with the machine and step-up transformer impedances. A network of up to 250 lines may be represented in SRPRES, and up to five sets of generator data may be entered.

System Data

The system elements which are used for SRPRES input data are represented in the following manner:

1. All long transmission lines with voltages of 230 kV or higher are represented by one or more "pi" equivalents.
2. Series compensation is represented as a percent of the line inductive reactance.
3. All short lines are represented by lumped R-L-C equivalents.

4. Transformers are represented the same as short lines. It is important that the representation of the generator step-up transformer be as accurate as possible.

5. Machines in the system may be represented by their short circuit equivalent or with the induction generator effect included. The induction generator model of a machine is represented by resistance and reactance versus frequency, as shown in Figure 23. The armature resistance of the machine is also added to these impedances. Generator manufacturers will provide this data, but it must be in the appropriate form for the frequency scanning program. SRPRES assumes the values are based on variable stator frequency and fixed rotor speed of 60 Hz.

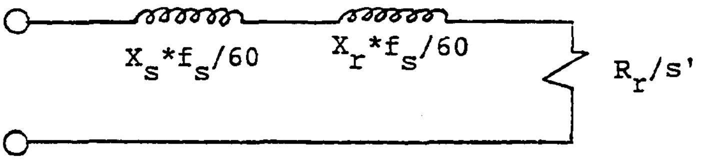

where f_s = stator current frequency,
f_o = freq. corresponding to average rotor speed,
$s' = (f_s - f_o)/f_s$

FIGURE 23 - INDUCTION GENERATOR MODEL FOR WESTINGHOUSE GENERATOR

Model Testing

RESOUT, the frequency scanning program conceived by General Electric, modified by Southern California Edison and Arizona Public Service (APS) and now used by Salt River

Project (SRP), was tested by APS using two separate sets of data obtained from the City Of Los Angeles (LADWP). Results were compared with the results of LADWP, which used the same set of data on their own program. Maximum deviation between output of the two programs was found to be 3 percent. In most of the frequency range, however, the deviation was less than 0.1 percent.

Determination of System Equivalents

The frequency scan program can be used to obtain a system equivalent representation in the following manner:

1. Run a frequency scan of a known system, with the study bus being the bus at which the desired system equivalents are sought. The frequency scan plot will show the equivalent impedances as a function of frequency looking into the system.
2. Guess on the equivalent resistance and reactance values for the desired system. Put these values in the frequency scan input data as an equivalent impedance to ground.
3. Run the frequency scan with the assumed impedances and compare to the known system frequency scan plot. The representative impedance should yield a frequency scan plot similar in magnitudes and shapes as the known system.

4. Modify the equivalent resistance and reactance, as necessary, to obtain a plot similar to that for the known system.

REFERENCES AND SELECTED BIBLIOGRAPHY

I. General Discussion of SSR

1. J. W. Butler and C. Concordia, "Analysis of Series Capacitor Application Problems," AIEE Transactions, Vol. 56, August 1937, pp. 975-988.

2. L. A. Kilgore, L. C. Elliott and E. R. Taylor, Jr., "The Prediction and Control of Self-Excited Oscillations Due to Series Capacitors in Power Systems," IEEE Transactions on Power Apparatus and Systems, Vol. PAS-90, No.3, May/June 1971, pp. 1305-1311.

3. J. W. Ballance and S. Goldberg, "Subsynchronous Resonance in Series Compensated Transmission Lines," IEEE Transactions on Power Apparatus and Systems, Vol. PAS-92, No. 5, September/October 1973, pp. 1649-1658.

4. IEEE Standard Dictionary of Electrical and Electronics Terms, second ed., 1977.

5. IEEE Subsynchronous Resonance Working Group, "Terms, Definitions and Symbols for Subsynchronous Oscillations," IEEE Transactions on Power Apparatus and Systems, Vol. PAS-104, No.6, June 1985, pp. 1326-1334.

II. Induction-Machine Effects

6. H. M. Rustebakke and C. Concordia, "Self-Excited Oscillations in a Transmission System Using Series Capacitors," IEEE Transactions on Power Apparatus and Systems, Vol. PAS-89, No. 7, September/October 1970, pp. 1504-1512.

7. C. E. J. Bowler, D. N. Ewart and C. Concordia, "Self-Excited Torsional Frequency Oscillations with Series Capacitors," IEEE Transactions on Power Apparatus and Systems, Vol. PAS-92, No. 5, September/October 1973, pp.1688-1695.

III. Torsional Torque Oscillations

8. C. Concordia, J. B. Rice and C. E. J. Bowler, "Subsynchronous Torques on Generating Units Feeding Series Capacitor Compensated Lines," Proceedings of the American Power Conference, Vol. 35, 1973, pp. 1129-1136.

9. D. N. Walker, C. E. J. Bowler, R. L. Jackson and D. A. Hodges, "Results of Subsynchronous Resonance Test at Mohave," IEEE Transactions on Power Apparatus and Systems, Vol. PAS-94, No. 5, September/October 1975, pp. 1878-1889.

10. R. G. Farmer, Eli Katz and A. L. Schwalb, "Navajo Project Report on Subsynchronous Resonance Analysis and Solutions," IEEE Transactions on Power Apparatus and Systems, Vol. PAS-96, No.4, July/August 1977, pp. 1226-1232.

IV. Methods of SSR Analysis

11. M. C. Hall, R. L. Daniels and D. G. Ramey, "A New Technique for Subsynchronous Resonance Analysis and an Application to the Kaiparowits System," IEEE Transactions on Power Apparatus and Systems, Vol. PAS-96, No. 4, July/August 1977, pp. 1251-1255.

12. IEEE Subsynchronous Resonance Task Force, "First Benchmark Model for Computer Simulation of Subsynchronous Resonance," IEEE Transactions on Power Apparatus and Systems, Vol. PAS-96, No. 5, September/October 1977, pp. 1565-1572.

13. L. A. Kilgore, D. G. Ramey, and M. C. Hall, "Simplified Transmission and Generation System Analysis Procedures Subsynchronous Resonance Problems," IEEE Transactions on Power Apparatus and Systems, Vol PAS-96, No. 6, November/December 1977, pp. 1840-1846.

14. B. L. Agrawal and R. G. Farmer, "Use of Frequency Scanning Techniques for Subsynchronous Resonance Analysis," IEEE Transactions on Power Apparatus and Systems, Vol. PAS-98, No. 2, March/April 1979, pp. 341-348.

15. M. B. Hughes, R. W. Leonard, and T. G. Martinich, "Measurement of Power System Subsynchronous Driving Point Impedance and Comparison with Computer Simulations," IEEE Transactions on Power Apparatus and Systems, Vol. PAS-103, No. 3, March 1984, pp. 619-630.

16. IEEE Subsynchronous Resonance Working Group, "Second Benchmark Model for Computer Simulation of Subsynchronous Resonance," IEEE Transactions on Power Apparatus and Systems, Vol. PAS-104, No. 5, May 1985, pp. 1057-1066.

17. G. D. Jennings, R. G. Harley and D. C. Levy, "Sensitivity of Subsynchronous Resonance Predictions to Turbo-Generator Modal Parameter Values and to Omitting Certain Active Subsynchronous Modes," IEEE Transactions on Energy Conversion, Vol. EC-2, No. 3, September 1987, pp.470-479.

V. Resistance of Conductors

18. H. B. Dwight, "Skin Effect in Tubular and Flat Conductors," AIEE Transactions, Vol. 37, Part II, 1918, pp. 1379-1403.

19. H. B. Dwight, "Skin Effect and Proximity Effect in Tubular Conductors," AIEE Transactions, Vol.41, 1922, pp. 189-198.

20. J. Zaborszky, "Skin and Spiraling Effect in Stranded Conductors," AIEE Transactions, Vol. 72, Part III, August 1953, pp.599-603.

21. W. A. Lewis and P. D. Tuttle, "The Resistance and Reactance of Aluminum Conductors, Steel Reinforced," AIEE Transactions, Vol. 77, Part III, February 1959, pp. 1189-1215.

22. Task Force of the IEEE Working Group on Calculation of Bare Overhead Conductor Temperatures, "AC Resistance of ACSR - Magnetic and Temperature Effects," IEEE Transactions on Power Apparatus and Systems, Vol. PAS-104, No. 6, June 1985, pp. 1578-1584.

23. Standard Handbook For Electrical Engineers, eleventh ed., McGraw-Hill Book Co., 1978, pp.4-5 to 4-79.

24. Electric Power Research Institute, Transmission Line Reference Book, second ed., 1982, p. 110.